

Chapter 5

STUDIES OF 1-AZACARBAZOLE IN BULK PROTIC SOLVENTS – I. DIOLS

5.1 Introduction

The study of excited-state tautomerism of 1-azacarbazole (1AC) in isolated hydrogen-bonded complexes has demonstrated that the proton-transfer is rapid [Chapter 4]. Although it is generally assumed that some hydrogen-bonded complex is necessary for promoting the excited-state tautomerization in bulk protic solvents, a molecular-level description of the reaction mechanism and identification of a rate-determining step continue to be discussed for the bulk protic solvents.¹⁻³⁷ Early work established that protic solvents catalyze the tautomerization reactions,¹⁻⁸ and noted the remarkable connection between the activation energy of the reaction and that of the bulk viscosity of alcohols, a connection that was interpreted to mean that large-amplitude molecular motion controls the reaction.^{5,6} At that time, neither the geometric structure^{5,7} nor the hydrogen-bonding strength^{2,5,7} of the alcohol solvents were deemed important for controlling the reaction.

Kinetic models of this reaction advanced with the advent of time-resolved measurements of sufficient resolution to monitor the entire reaction.³⁸ Many of the early experiments on 7-azaindole (7AI) in bulk alcohols indicated that solvent dynamics was

one important factor in controlling the rate of the reaction.^{16,29,34} Some workers also noted that the proton-transfer rate was strongly correlated to the hydrogen-bonding strength or acidity of the alcohol solvents.^{33,16} A dominant theme in the description of the reaction was that the mechanism could be understood as a two-step process.^{34,33,16,29}

The following examples illustrate the two-step models proposed for the mechanism. Differences among the interpretations arise mainly from whether static or dynamic aspects of the first step control the reaction. In the first direct measurement of the excited-state proton-transfer rate of 7AI in alcohols, McMorow and Aartsma³⁴ proposed a model invoking two types of solvent configurations to explain two lifetimes growing into the decay of 7AI tautomer fluorescence at 510 nm. A pre-formed, cyclically hydrogen-bonded complex was proposed to enable instantaneous proton transfer (20 ps in methanol), while other configurations exhibited a slower response (165 ps in methanol) as solvent-solute reorganization dynamics determined the rate of attaining the cyclically hydrogen-bonded complex needed for the proton-transfer event. Later measurements were unable to reproduce the amplitude of the rise time in the tautomer fluorescence in alcohols attributed to this intrinsic proton-transfer step.^{16,29,33,39} Even with subpicosecond resolution, the ultrafast component proposed by McMorow and Aartsma has not been observed.^{25,26} Two years later, Varma and coworkers explained the reaction as a two-step process in which a tunneling proton transfer (for the two protons) followed the formation of a cyclically hydrogen-bonded 7AI-alcohol complex.³³ This kinetic model satisfactorily accounted for their observations of a temperature-independent kinetic isotope effect and of rate dependence on the acidity of

the alcohols rather than on viscosity or solvent aggregation.³³ Moog and Maroncelli¹⁶ retained and modified the two-step model of McMorrow and Aartsma³⁴ in order to explain an interesting¹¹ temperature dependence of the kinetic isotope effect on the reaction rate.

Study of the excited-state tautomerization of 7AI and 1AC has continued at a fervent pace. The interpretation of the reaction mechanism has evolved and no longer maintains that “solvation dynamics” is relevant in the discussion.^{10,11,20} The issue of the temperature dependence of the reactions of 7AI and 1AC in alcohols was revisited by Maroncelli *et al.*,^{10,11,13,14} and the observed reaction rate is currently modeled by

$$k_{\text{obs}} = k_{\text{PT}} \exp(-\Delta G/kT) \quad (5.1)$$

where k_{PT} is the intrinsic proton-transfer rate in a proper configuration and ΔG is the equilibrium solvation free energy needed to achieve that cyclic complex.^{10,11} The essence of this model is very similar to that originally proposed by Varma and coworkers one decade earlier.³³ Advocating a different physical picture, Petrich and coworkers recently argued that the rate-determining step involves the actual proton-transfer rather than the solvent reorganization required to form the necessary cyclic hydrogen-bonded complex.²⁰ The challenge faced by all models is the decomposition of the one observed rate into two or more contributions from likely physical processes occurring in solution.

Linear correlations of the proton-transfer rates of 7AI and 1AC with some measure of the hydrogen-bond donating ability of the neat protic solvents were introduced in Chapter 3. These linear free-energy relationships are consistent with the general decomposition of the observed rate into some solvent independent intrinsic rate

and a rate factor depending on the solvent. Interesting deviations from the linear relationships observed in bulk alcohols have been noted for highly polar and viscous solvents such as diols, water, and amides.⁴⁰ Do these deviations suggest that the excited-state of 7AI or 1AC is depopulated via alternative pathways? This question has been explored at length for 7AI in water without convergence to a clear understanding.^{1,2,15,18-32,36} Since the photophysics and photochemistry of 1AC is similar to that of 7AI, experimental studies on the excited-state tautomerism of 1AC in these bulk protic solvents were undertaken in an attempt to understand the origin of these differences.

5.2 1AC in Diols

Noted in earlier studies of the excited-state tautomerism of 7AI and 1AC,^{16,13} the measured reaction rates in diols and water appear to be anomalously slow when compared to the rates of alcohols plotted on the $E_T(30)$ polarity scale (*cf. Figure 3.2*). If the reaction rate is determined by some form of solvent dynamics, it might be expected to be much slower in the very viscous diols. However, the reported rates do not correlate in any simple way with bulk viscosities or alternative measures of solvation dynamics.^{33,16,13} To develop a better understanding of these slow reaction rates, the temperature dependence of excited-state tautomerization of 1AC was examined in ethylene glycol, ethylene glycol-D₂, and propylene glycol over the range 1 °C - 70 °C. Experiments on 7AI in ethylene glycol were also repeated to provide a base of comparison with earlier results.¹⁶

5.2.1 Temperature Dependence of 1AC Lifetimes

At temperatures above 40-50 °C, the time-resolved emission of 1AC in diols indicates kinetics consistent with an irreversible proton-transfer model as described in Chapter 3. A minor component to describe possible impurity fluorescence (<5%, $\tau \sim 5$ ns) and a component to account for a dynamic Stokes shift (<100 ps) in the normal region are added to this model. For example at 70 °C in ethylene glycol (EG), the 1AC normal emission decays in 430 ps as the tautomer emission exhibits a decay (reaction) time of 420 ps and a rise (tautomer deactivation) time of 250 ps. (Recall from Chapter 3 that the rise time of the tautomer species does not necessarily correspond to the growth of the product during the reaction. Instead, it is the relative rates of the reaction and of the tautomer deactivation that determine the correct interpretation of the tautomer rise time.)

At or below room temperature, however, the kinetics become more complicated. For reference, at 20 °C in ethylene glycol (EG) the 1AC normal emission decays in 1.01 ns as the tautomer emission exhibits a decay (reaction) time of 1.05 ns and a rise (tautomer deactivation) time of 320 ps. The complications become more apparent when the lifetimes are plotted as a function of temperature. A plot of the tautomer rise (deactivation) times does not increase steadily with decreasing temperature as might be anticipated (*Figure 5.1*), a feature also present in the temperature dependence for ethylene glycol-D₂ (*Figure 5.2*) and propylene glycol (*Figure 5.3*). Two alternative fits of the tautomer emission are explored in order to assess the significance of these observations. In the first alternative fit, the term to model possible impurity emission is constrained to a long nanosecond lifetime. This affects little change in the behavior of

the tautomer rise (deactivation) time for 1AC. In the second alternative fit, the tautomer rise (deactivation) times at high temperatures are extrapolated to lower temperatures (as indicated in *Figure 5.1*, *Figure 5.2* and *Figure 5.3*) and constrained with the impurity term while fitting the emission decay. At lower temperatures, an additional component is then needed to fit the tautomer rise, and the overall effect does lengthen the tautomer rise (deactivation) times. Physical interpretation of the biexponential rise times may lack warrant, however, since a weighted average value of the tautomer rise times differs little from that fit without constraints. (See *Table 5.1*, *Table 5.2*, *Table 5.3*, *Table 5.6*, *Table 5.7*, and *Table 5.8* for summaries of the temperature studies of 1AC in ethylene glycol.)

In retrospect, it is not clear that these alternative fits for 1AC in ethylene glycol provide useful perspective on the reaction and especially the tautomer rise (deactivation) times at low temperatures. The various lifetimes of multiexponential fits to the emission data may not necessarily have a unique physical interpretation. Nevertheless, good estimates of the reaction and tautomer deactivation rates are needed for modeling the reaction in general. The extraction of these parameters is complicated by the apparent slowness of the reaction rate especially when compared to the normal deactivation rate k^N observed in aprotic solvents. This general consideration is discussed in the next section before we present the best estimates for the reaction rates in diols.

5.2.2 Reaction Rate Determination with Possible k^N Contamination

The irreversible proton-transfer kinetic scheme requires $k_{\text{rxn}} \gg k^N$ in order to interpret the observed rate k_{obs} as the reaction rate k_{rxn} . Because the 1AC observed rates k_{obs} are close to the 1AC normal deactivation rates k^N , a correction may need to be applied to the observed rates in order to account for this alternative pathway of deactivation (k^N) and to extract the true reaction rate. Although this correction is simply $k_{\text{rxn}} = k_{\text{obs}} - k^N$, the actual determination of k^N may be troublesome. Three possibilities are explored to estimate the magnitude of k^N and to assess the change between the observed rate and the reaction rate.

(Method 1) One could assume that the deactivation rate k^N of the normal species in protic solvents is equal to that in aprotic solvents, and the observed rates could be corrected using the aprotic values of k^N . For example at room temperature, $k^N = (1.1 \pm 0.2) \times 10^8 \text{ s}^{-1}$ for the aprotic solvents (*Table 2.3*). When this correction is applied to the protic solvents at room temperature (*Table 2.3*), many corrected reaction rates are slower by ~10-20% of the observed rates, with notable exceptions including methanol-OD (~ 30%) and N-methylformamide (~ 50%).

(Method 2) The reaction rate may be estimated directly from the expression derived in Chapter 3,

$$k_{\text{rxn}} = (k_{\text{rad}}^N / k_{\text{rad}}^T) (\varphi^T / \varphi^N) k^T, \quad (5.2)$$

and compared the observed rate to determine k^N . For this comparison at room temperature, the average value of $k_{\text{rad}}^N / k_{\text{rad}}^T = 9 \pm 1$ for six protic solvents is used in the calculation of the reaction rates for all protic solvents since this ratio is assumed to be

representative of all of them (*Table 2.3*: MeOH, 1-PrOH, 1-PeOH, 2-PrOH, BzOH, and TFE). Although this approach predicts negative values of k^N , within experimental uncertainty the rates of many protic solvents are in agreement with k^N determined from the aprotic solvents. Exceptions include methanol-OD, 1-pentanol, ethylene glycol, formamide and N-methylformamide. Many estimated reaction rates k_{rxn} are slightly faster than the observed rates, but with the exception of t-butanol and ethylene glycol, agree within experimental uncertainty.

The comparisons in Methods (1) and (2) are made using data recorded at room temperature. The normal deactivation rate k^N does depend on the temperature of the experiment, so k^N must be estimated at each temperature at which the correction to the observed rate is made. The tautomer deactivation rate k^T also depends on temperature and must be measured directly in each protic solvent. The concern over k^N is especially important in interpreting the isotope and low temperature studies. The correction of rates at low temperatures is summarized elsewhere,^{13,14} but the data of 1AC in ethylene glycol is reexamined here with additional detail. The following third method of analysis provides one means for estimating the temperature dependence of k^N .

(Method 3) The following analysis is summarized in *Table 5.6*, *Table 5.7*, and *Table 5.8*. Method (3) is like Method (2) except that the temperature dependence of the quantum yield ratios ϕ^T / ϕ^N are determined directly from normalized emission spectra.⁴¹ The total quantum yields for 1AC in ethylene glycol at the temperatures in this experiment are estimated by scaling the relative quantum yields to the absolute quantum yield $\phi=0.019$ at 295 ± 2 K from *Table 2.3*. The quantum yields for 1AC in ethylene

glycol-D₂ are estimated in a similar fashion. Although a quantum yield for 1AC in ethylene glycol-D₂ is not available in *Table 2.3*, it is estimated from the quantum yield of 1AC in ethylene glycol by assuming that 1AC has the same normal radiative rate in the deuterated solvent. Thus, for 1AC in ethylene glycol-D₂ the quantum yield is estimated $\phi=0.051$ at 295 ± 2 K (based on an isotope effect of 2.7 in the normal lifetime). The radiative rates are determined from the quantum yield estimates and the fluorescent lifetimes of the normal and tautomer species. In both these solvents, the normal radiative rate is constant over the range 1-70 °C with $k_{\text{rad}}^{\text{N}} = 1.7 \times 10^7 \text{ s}^{-1} \pm 2\%$. The tautomer radiative rates are dependent on the method of fitting the time-resolved emission as noted above, and they are constant or slowly increasing with decreasing temperature (assuming a complete and irreversible reaction). The ratio $k_{\text{rad}}^{\text{N}} / k_{\text{rad}}^{\text{T}}$ is reasonably constant over the entire temperature range, although it is almost a factor of two smaller than the average value for the six protic solvents chosen in Method (2). The estimates for k^{N} using the “second alternate fit” are in best agreement with the aprotic rate $k^{\text{N}} = 1.1 \times 10^8 \text{ s}^{-1}$. With $k_{\text{rad}}^{\text{N}} / k_{\text{rad}}^{\text{T}} \sim 5$, approximately one-half of the predicted values of k^{N} are negative (not realistic), but the predicted reaction rates are within 20% of the observed rates. With $k_{\text{rad}}^{\text{N}} / k_{\text{rad}}^{\text{T}} \sim 9$, the predicted values of k^{N} are all significantly negative (not realistic), and the predicted reaction rates are all significantly larger than the observed rates.

The results of Methods (2) and (3) suggest that either the ratio $k_{\text{rad}}^{\text{N}} / k_{\text{rad}}^{\text{T}}$ displays a modest solvent (*e.g.*, polarity) dependence, or that extracting lifetimes with accurate physical interpretation is difficult as the reaction slows. Without a means of independently determining k^{N} in protic solvents at the temperatures studied, and

considering the observations noted above, the rates k_{rxn} and k^{T} will be uncertain by at least 10-20%. The best estimates for rates and isotope effects for the temperature studies will include the quantum yield correction described in Method (3) using the ratio $k_{\text{rad}}^{\text{N}}/k_{\text{rad}}^{\text{T}}$ determined at high temperatures.

5.2.3 Temperature Dependence of 1AC Reaction Rates in Diols

The best estimates of the reaction rates (based on the second alternative fit) are summarized in *Figure 5.5*. Unlike the temperature dependence of 7AI in bulk alcohols, the estimated activation energy for the reaction is only ~60% of that for viscosity (*Table 5.11*). The isotope effect appears to be largely independent of temperature. This temperature-independent isotope effect is similar to that for the related tautomerization in bulk alcohols except that its magnitude is slightly smaller (see Chapter 7).^{11,13}

5.2.4 Temperature Dependence of 7AI in Diols

The temperature dependence of the 7AI reaction in ethylene glycol and propylene glycol is similar to that observed for 1AC. At high temperatures the kinetics are consistent with the irreversible proton-transfer scheme: the normal fluorescence of 7AI decays with lifetime of ~170 ps as the tautomer emission appears with a 140 ps rise (reaction) time before decaying (deactivation) with a lifetime of 450 ps. In diols, the excited-state reaction for 7AI is three times faster than for 1AC. Note that this example for 7AI is consistent with the usual interpretation of the decay and rise components in the

time-resolved fluorescence of a two-state reaction. The normal form of the molecule disappears (emission decay) at the rate of the reaction while the tautomer form of the molecule appears (emission rise) at the rate of the reaction before disappearing (emission decay) at a different rate. This interpretation stands in contrast to that for 1AC.

Below room temperature, the kinetics are again more complicated. The alternative fitting models described for 1AC reactions in diols did provide insight into the interpretation of the excited-state lifetimes observed for 7AI in the viscous diols. The most striking illustration involves the reaction in propylene glycol (*Figure 5.4*). The tautomer rise (reaction) times do not increase monotonically with decreasing temperature as might be expected. If the high temperature tautomer decay (deactivation) times are extrapolated to lower temperatures and constrained (the second alternative fit model), then the refit rise (reaction) times do increase monotonically. At low temperatures, the rise (reaction) and decay (deactivation) times are then nearly equal. Since this model fits the data as well as the original fit, it suggests that quantitative measurements of the interesting interplay between the reaction rate and tautomer deactivation rate are obscured in the data. This near crossover in interpretation of the tautomer rise (reaction to deactivation) and decay (deactivation to reaction) times is consistent with the model for the reaction of 7AI in water, where the tautomer decay time was interpreted as the measure of the reaction time.¹⁵

Possible corrections to the time-resolved fluorescence of 7AI in ethylene glycol were not as severe as those described for the reaction in propylene glycol. (See *Table 5.1*, *Table 5.4*, and *Table 5.5* for summaries of fits.) Biexponential rise (reaction) times

for 7AI in ethylene glycol were observed at low temperatures. An effort to fit these data using a nonexponential model was unsuccessful.⁴² The best estimates for the reaction times using the second alternative fit with corrections based on relative quantum yields are compared to the 1AC results (*Figure 5.5*). Like 1AC, the Arrhenius activation energy of the 7AI reaction is ~60% of that for viscosity (*Table 5.11*), and the isotope effect is largely independent of temperature, consistent with earlier reports.¹¹

5.2.5 Comparison of 7AI Reaction Rates in Diols to Literature Values

Petrich and coworkers have reported lifetime measurements for the normal form of 7AI in ethylene glycol and propylene glycol.²⁰ In this work emission was collected over the entire normal band (320 - 460 nm) and was fit to a sum of two exponentials $F(t) = a_1 \exp(-t/\tau_1) + a_2 \exp(-t/\tau_2)$. Their results are summarized, $N(t) = a_1 (\tau_1) + a_2 (\tau_2)$:²⁰

$$\text{EG (20 }^\circ\text{C)} \quad N(t) = 0.31 (0.141 \text{ ns}) + 0.69 (0.461 \text{ ns})$$

$$\text{PG (20 }^\circ\text{C)} \quad N(t) = 0.31 (0.197 \text{ ns}) + 0.69 (0.816 \text{ ns})$$

The shorter lifetime was interpreted as the reaction time, and the longer lifetime was interpreted as emission from 7AI in a “blocked” form of solvation. The time dependencies of the normal bands measured by Petrich and coworkers are similar to those recovered in the experiments reported in this dissertation. In order to compare the results directly, a biexponential fit is constructed from weighted averages of corresponding terms in the multiexponential fit to the normal emission at 370 nm:

$$\text{EG (20 }^\circ\text{C)} \quad N(t) = 0.32 \langle 0.084 \text{ ns} \rangle + 0.68 \langle 0.43 \text{ ns} \rangle$$

$$\text{PG (20 }^\circ\text{C)} \quad N(t) = 0.55 \langle 0.098 \text{ ns} \rangle + 0.45 \langle 0.89 \text{ ns} \rangle$$

We interpret these lifetimes differently than Petrich and coworkers:²⁰ the short time is attributed to a dynamic Stokes shift,⁴³ and the long (mean) time is attributed to the reaction time.

Our measurements of the tautomer emission at 560 nm reveal average rise times that are faster than the (long) decay times of the normal emission:

$$\text{EG (20 }^\circ\text{C)} \quad T(t) = - 8.41 \langle 0.32 \text{ ns} \rangle + 9.41 \langle 0.77 \text{ ns} \rangle$$

$$\text{PG (20 }^\circ\text{C)} \quad T(t) = -10.1 \langle 0.62 \text{ ns} \rangle + 11.1 \langle 0.95 \text{ ns} \rangle$$

In the simple irreversible proton-transfer scheme for 7AI, the normal emission decay (reaction) time should be equal to the measured tautomer rise (reaction) time. As noted above, the reaction of 7AI in propylene glycol may be difficult to measure directly because of ambiguity in the lifetimes obtained from the fits to the emission. The reaction of 7AI in ethylene glycol may more closely approach an irreversible proton-transfer scheme. If weighted average normal lifetimes are calculated from the data of Petrich and coworkers,²⁰ their agreement with the mean reaction (rise) times measured in the tautomer is good. It may be possible that our measurements are unable to separate completely a time constant for the dynamic Stokes shift so that the averaged short lifetime $\langle \tau_1 \rangle$ includes some contribution from reacting 7AI. It is unlikely that two or more distinct populations involving these proton-transfer molecules should exist in solution based on recent experiments and simulations which indicate the short-lived nature of hydrogen-bonded complexes in protic solvents.^{44,10}

5.3 Temperature Study of 1AC in Benzyl Alcohol

Since the observed rates of 1AC are anomalously fast in benzyl alcohol on the basis of the $E_T(30)$ correlation, a brief study of the temperature dependence of the reaction was undertaken to estimate the Arrhenius activation energy. The data are summarized in *Figure 5.6* and *Table 5.9*. The observed lifetimes of the normal and tautomer species are difficult to interpret uniquely at room temperature. At temperatures above 45 °C, the lifetime of the normal species matches the rise time of the tautomer species suggesting that the rise time is the reaction time. This is like the “usual” interpretation for a two-state reaction as observed for 7AI in most protic solvents. At temperatures below 15 °C, non-exponential behavior is observed, and the lifetime of the normal species approaches the decay time of the tautomer species. This is like the interpretation for a two-state reaction as observed for 1AC in most of the protic solvents. This crossover in interpretation is similar to the observed kinetics for 7AI in propylene glycol and water, in which the decay time rather than the rise time of the tautomer’s emission is taken as a measure of the reaction rate. The Arrhenius activation energy of the reaction is only 50-60% of that for viscous flow⁵⁰ determined over the temperature range 25 °C - 65 °C. The best estimate for the reaction time of 1AC in benzyl alcohol at room temperature is 0.29 ± 0.02 ns.

5.4 Interpretation of the Anomalous Low Temperature Behavior

The more complicated kinetics (*i.e.*, kinetics not conforming to a simple two-state model) observed at low temperatures in the diols has also been noted in other solvent systems. For 7AI in 1-propanol and 1-butanol, like 7AI in propylene glycol, the tautomer rise (reaction) times do not increase monotonically with decreasing temperature but instead exhibit a turnover in the region 200-230 K.¹⁴ For 1AC in methanol, the tautomer rise (deactivation) times approach a constant value in the region below 200 K, and for 1AC in 1-propanol the tautomer rise (deactivation) times are nearly constant over the range 200-300 K (with much more scatter in the 1AC/PrOD results).¹³ For 1AC in benzyl alcohol and in N-methylformamide (Chapter 6), similar behavior is observed near 0 °C.

In an effort to identify possible underlying molecular phenomena leading to these observations, we examined several simple expressions related to models for translational and rotational molecular motion. Random molecular motion may transport matter from one part of a system to another by the process named diffusion. The Stokes-Einstein law is a hydrodynamic theory that models the diffusion constant D of a spherical molecule with radius r in a (continuous) solvent medium with viscosity η :⁴⁵

$$D = \frac{k_B T}{6\pi\eta r} \quad (5.3)$$

The ratio η / T was examined for each of the solvents noted above over the range of experimental temperatures to look for a common value that might be suggestive of the influence of (random) molecular motions controlling the reaction. The time scale of

molecular rotations may also be estimated from hydrodynamic theory. The rotational times of 1AC and 7AI in these solvents are calculated using

$$\tau_{\text{rot}}^{(2)} = C_{\text{obs}} f V_p \eta / k_B T, \quad (5.4)$$

where the constants C_{obs} and f are estimated from a recent study⁴⁶, and the volume of the solute V_p and the viscosity η are determined using published algorithms.⁴⁷⁻⁵⁰

Table 5.10 summarizes temperature-normalized solvent viscosities and the estimated rotation times and their dependence on temperature and solvent for 1AC and 7AI. The shaded regions of *Table 5.10* indicate regions in which the observed kinetics begin to show deviations from the simple irreversible proton-transfer scheme. In the viscosity data, the deviations for 1AC begin to appear at an effective (room temperature) viscosity of approximately 2.5 cP in methanol, 1-propanol and N-methylformamide. The deviations for 7AI begin to appear at an effective (room temperature) viscosity of approximately 14 cP in ethylene glycol and 1-propanol. It is interesting to note that the effective diffusion constant based on the effective viscosity for 1AC is nearly five times greater than that for 7AI, perhaps corresponding to the reaction times for which 1AC is about five times greater than 7AI. (The estimates of the effective diffusion constants require the approximate radii of 1AC and 7AI which are estimated in Chapter 2 to be 3.3 Å and 2.9 Å, respectively.)

In the molecular rotation time data, the estimated rotation times of 7AI and 1AC in the different protic solvents are 100-200 ps and ~50-200 ps at the onset of deviations, respectively. Even though these times are inexact and may require rescaling, these times are suggestive of a regime in which molecular motion does influence the reaction or the

deactivation of the tautomer species. This molecular motion may involve interactions between the proton-transfer molecule and the protic solvent molecules or just among the protic solvent molecules.⁵¹ Since the ratios of reaction times to rotation times are not obviously constant at the onset of deviations [*e.g.*, $\tau_{\text{rxn}} / \tau_{\text{rot}} \sim 40$ (1AC in 1-PrOH), 10 (7AI in 1-PrOH), 5 (1AC in EG), and 3 (7AI in EG)], the limiting molecular interactions may be occurring among the solvent molecules.

The correlation of rotation times with the onset of the low temperature anomalous behavior prompted a more careful examination of the time-scales of possible molecular dynamics. The temperature dependence of the dielectric relaxation of the primary alcohols and ethylene glycol provides insight in this matter.⁵² The primary alcohols such as 1-propanol exhibit three dielectric relaxation times, and the dielectric dispersion data of ethylene glycol may be decomposed into two times.⁵² The relaxation times are ordered τ_1 (~50+ ps) > τ_2 (~20-40 ps) > τ_3 (~2 ps), with τ_1 making the dominant contribution to the total dispersion.⁵² Following the interpretation of Garg and Smyth, the first relaxation time is attributed to rotation of alcohol molecules in clusters, the second time is attributed to rotation of free alcohol monomers, and the shortest time is attributed to rotation of the -OH group.⁵² Berg and coworkers have demonstrated that the dielectric relaxation (τ_1 or τ_D) is proportional to the dynamics of hydrogen-bond formation,⁴⁴ an important step prior to the breaking of covalent bonds in the proton-transfer reaction. Berg and coworkers note that the lifetime of a hydrogen bond is not simply the time required to break a hydrogen bond, but the time involved in the equilibration of the solvent about the newly broken or formed hydrogen bond.⁴⁴

In earlier studies on 7AI, no good correlations were reported between the longitudinal relaxation times (τ_L , or other measures of solvation dynamics) and the reaction times (τ_{rxn}).¹⁶ However, an interesting correlation exists for many solvents between the dielectric relaxation times τ_1 and the reaction times τ_{rxn} . (The dielectric relaxation times τ_1 used here are summarized in *Table 5.12*.) The correlations for 1AC in methanol, ethylene glycol, a portion of 1-propanol, and formamide and the correlations for 7AI in methanol and ethylene glycol are illustrated in *Figure 5.7*. Similar correlations have been observed for 1AC in 1-propanol, water, and N-methylformamide and for 7AI in 1-propanol and 1-butanol. For each of these solvents, the reaction time and relaxation time show a direct relationship over the range of temperatures studied. The correlation plots of the observed reaction rates and the dielectric relaxation times for 1AC and 7AI in methanol/methanol-OD and ethylene glycol/ethylene glycol-D₂ (*Figure 5.8*) remind us that other factors are important in modeling the reaction. In this example (*Figure 5.8*), the isotope effects attributed to the intrinsic proton-transfer step cause the offsets of the correlation curves.

The plots in *Figure 5.7* and *Figure 5.8* are interpreted to indicate that the reactions of 7AI or 1AC in methanol and ethylene glycol are quite similar based on the overlap of the correlations. This agreement may not be surprising since the structure of ethylene glycol is like two bonded methanol units. On the other hand, the lack of correlation among the very different solvents emphasizes the involvement of additional factors in determining the reaction rates. The observed reaction time τ_{rxn} is currently modeled as

the product of an intrinsic proton-transfer time τ_{PT} and a solvent factor here denoted by the variable S :

$$\tau_{rxn} = \tau_{PT} S. \quad (5.5)$$

The solvent factor S will be interpreted liberally to include contributions from effects such as the solvent polarity S_{polarity} and the dynamics of hydrogen-bond formation $S_{\text{H-bond}}$:

$$\tau_{rxn} = \tau_{PT} S_{\text{H-bond}} S_{\text{polarity}}. \quad (5.6)$$

Above we noted that the dielectric relaxation τ_1 is proportional to the dynamics of hydrogen-bond formation,⁴⁴ $S_{\text{H-bond}} = \tau_1 S_{\text{H-bond}}'$, whose substitution into equation (5.6) yields the expression:

$$\tau_{rxn} = \tau_1 \tau_{PT} S_{\text{H-bond}}' S_{\text{polarity}}. \quad (5.7)$$

If the intrinsic proton transfer time and solvent factors $S_{\text{H-bond}}' S_{\text{polarity}}$ are the same or very similar for a group of solvents, then the reaction times for all such solvents should be directly related to the dynamics of hydrogen-bond formation. This may be the case for the reaction of 7AI in methanol and ethylene glycol and for the reaction of 1AC in methanol and ethylene glycol. On the other hand, if a factor such as the intrinsic proton transfer time differs, then the plots of the reaction times will be offset when plotted as a function of the dielectric relaxation times. This explains why the correlations for 7AI and 1AC in methanol and ethylene glycol do not overlap (different τ_{PT} arising from different molecules), why the correlations for 7AI and 1AC in protiated and deuterated solvent pairs do not overlap (different τ_{PT} arising from isotope effects), and why the correlations for 1AC in the various solvents may not overlap (different S).

To view the correlation between the reaction time and the dielectric relaxation time in a slightly different format, *Figure 5.9* illustrates the ratio τ_l / τ_{rxn} plotted on the $E_T(30)$ solvent polarity scale. This plot represents the reaction rate normalized by a measure of the cooperative hydrogen-bond dynamics as a function of solvent polarity. These normalized reaction times for the alcohols, ethylene glycol and water show an exponential dependence on this measure of polarity, consistent with the mathematical form of Equation (5.1). Furthermore, the points for ethylene glycol and water now lie along the same linear correlation for the primary alcohols with the $E_T(30)$ scale. (The reaction in water is also discussed in more detail in Chapter 6.)

Because the $E_T(30)$ polarity scale is a measure of hydrogen-bond strength based on the absorption of betaine dyes,⁵³ this scale is insensitive to the dynamics of hydrogen bonds. Of course, the dynamics of hydrogen bonds ultimately depend on potential barriers (a static property). It appears that the $E_T(30)$ scale does not probe such energetics well. When the effects of the hydrogen bond dynamics are removed from the reaction rates, then we observe the corrected rates' direct dependence on solvent polarity and hydrogen-bond strengths.

5.5 Conclusion

The original question driving this study of the reaction of 1AC in the diols was based on the interesting deviations of these reaction rates from the linear relationships observed for bulk alcohols plotted on the $E_T(30)$ scale. Do these deviations suggest that

the excited-state of 7AI or 1AC is depopulated via alternative pathways? Based on the correlation of the reaction times with the dielectric relaxation times, we conclude that the proton-transfer reaction in ethylene glycol is *not* intrinsically different than that observed in methanol. Rather, it is simply in a different regime determined by the dynamics of cooperative hydrogen-bond formation. Future study of the excited-state reaction of 7AI or 1AC in the alcohol / diol solvent pairs such as ethanol / 1,3-butanediol or ethanol / 1,4-butanediol may further support this hypothesis.

In the preceding analyses, good correlations were observed between the anomalous kinetics at lower temperatures and estimated rotation times, and between the reaction and (Debye) dielectric relaxation times, both of which are related to viscosity. And noted in *Table 5.11*, the Arrhenius activation energies for the reactions, the dielectric relaxation (τ_1), and viscosity are often similar in magnitude. As viscosity is also one measure of the solvent “friction” along the reaction coordinate,⁴⁴ future understanding of this concept may be able to untangle the physical mechanisms leading to these interesting correlations for the proton-transfer reactions. Until then, the data indicate that (dynamic) solvent effects related to the equilibration of broken or formed hydrogen bonds partially control the rate of the excited-state tautomerizations of 7AI and 1AC.

The present results do indicate that “solvation dynamics” or more specifically cooperative hydrogen-bonding dynamics is a significant part of the problem in the case of the proton-transfer reaction of 7AI or 1AC in ethylene glycol. When the observed rates are normalized by a measure of hydrogen-bond lifetimes,⁴⁴ the reactions of 7AI or 1AC in methanol and ethylene glycol may be compared on nearly equal footing. In

demonstrating that the 1AC reactions in the diols and water are not necessarily anomalous when plotted on the $E_T(30)$ solvent scale, however, a few new “anomalous” solvents were uncovered: 2-propanol, t-butanol, and glycerol. Interestingly, these secondary and tertiary alcohols also did not quite fit the model in the computer simulations by Mente and Maroncelli.¹⁰ Future work should address the reaction of 1AC and 7AI in these solvents.

The enthalpy changes measured experimentally refer to the differences in energy between a hydrogen-bonded state and a nonbonded state involving an incompletely solvated solvent molecule.⁴⁴ These enthalpy changes are consistent with the interpretation that the reaction activation energy for 7AI (and 1AC) is the enthalpy change in forming the cyclically hydrogen-bonded complex necessary for reaction.¹⁰ Such an interpretation provides an alternate picture for the large-amplitude solvent motion advocated earlier for controlling the excited-state proton-transfer rate, an interpretation based on the similarities between the Arrhenius activation energies for reaction and the temperature dependence of viscosity.^{5,6,16,29}

Table 5.1: Temperature Dependence of the Normal Emission of 7AI and 1AC in Ethylene Glycol

7AI / EG Normal				
Temperature (K)	$\langle a_1 \rangle$	$\langle a_2 \rangle$	$\langle \tau_1 \rangle$ ns	$\langle \tau_2 \rangle$ ns
275	0.21	0.79	0.072	0.68
283	0.28	0.72	0.065	0.59
294	0.32	0.68	0.084	0.43
303	0.30	0.70	0.055	0.32
314	0.27	0.73	0.044	0.26
323	0.25	0.76	0.042	0.21
333	0.24	0.77	0.037	0.18
343	0.20	0.80	0.048	0.17

7AI / EG-D ₂ Normal			
Temperature (K)		$\langle \tau_2 \rangle$ ns	IE
275		1.35	2.0
283		1.08	1.8
294		0.79	1.8
303		0.69	2.2
314		0.57	2.2
324		0.51	2.4
334		0.43	2.4
344		0.39	2.3

1AC / EG Normal				
Temperature (K)	$\langle a_1 \rangle$	$\langle a_2 \rangle$	$\langle \tau_1 \rangle$ ns	$\langle \tau_2 \rangle$ ns
274	0.27	0.73	0.09	1.75
283	0.53	0.47	0.03	1.37
293	0.24	0.76	0.06	1.01
303	0.45	0.55	0.06	0.82
314	0.35	0.65	0.03	0.66
323	0.34	0.66	0.02	0.55
333	0.43	0.58	0.02	0.49
344	0.40	0.60	0.02	0.43

1AC / EG-D ₂ Normal					
Temperature (K)	$\langle a_1 \rangle$	$\langle a_2 \rangle$	$\langle \tau_1 \rangle$ ns	$\langle \tau_2 \rangle$ ns	IE
275	0.37	0.64	0.1	4.6	2.6
283	0.33	0.68	0.09	3.6	2.6
293	0.29	0.72	0.06	2.8	2.7
303	0.32	0.68	0.03	2.37	2.9
314	0.38	0.62	0.02	1.99	3.0
323	0.46	0.54	0.01	1.75	3.2
334	0.45	0.55	0.02	1.59	3.3
344	0.51	0.49	0.008	1.51	3.6

Average lifetimes from multiexponential fits are presented as the best measurements of the observed rate. The slow times $\langle \tau_2 \rangle$ were separated from the more rapid times $\langle \tau_1 \rangle$ attributed to the dynamic Stokes shift. The kinetic isotope effect is defined as $IE = \langle \tau_2(D) \rangle / \langle \tau_2(H) \rangle$.

Table 5.2: Temperature Dependence of Tautomer Emission of 1AC in Ethylene Glycol

IAC / EG	Original Fit		Tautomer		τ_1 ns	τ_2 ns	τ_3 ns	τ_4 ns
T (K)	a_1	a_2	a_3					
274	-1.94	2.58	0.36		0.31		1.66	3.60
283	-2.71	3.71			0.30		1.42	
293	-3.10	4.10			0.31		1.07	
303	-5.99	6.99			0.31		0.83	
314	-7.01	8.01			0.29		0.66	
323	-9.64	10.64			0.28		0.56	
333	-9.55	10.55			0.26		0.49	
344	-11.29	12.29			0.24		0.42	

IAC / EG	Alt. Fit #1		Tautomer		τ_1 ns	τ_2 ns	τ_3 ns	τ_4 ns	$\langle I(570) \rangle$	$\langle \alpha(570) \rangle$	τ_{rxn} ns
T (K)	a_1	a_2	a_3	a_4							
274	-1.88		2.77	0.12	0.31		1.76	6	0.032	5.48	1.43
283	-2.68		3.66	0.03	0.30		1.40	6	0.041	5.28	1.10
293	-3.16		4.12	0.04	0.32		1.05	5	0.049	6.34	0.98
303	-6.03		7.02	0.01	0.31		0.83	5	0.056	6.71	0.82
314	-7.27		8.26	0.01	0.30		0.65	5	0.065	7.12	0.69
323	-9.57		10.56	0.01	0.28		0.55	5	0.069	7.47	0.61
333	-9.83		10.82	0.01	0.26		0.48	5	0.071	7.66	0.55
344	-11.64		12.62	0.01	0.25		0.42	5	0.076	7.76	0.48
										$\langle 6.73 \rangle$	

IAC / EG	Alt. Fit #2		Tautomer		τ_1 ns	τ_2 ns	τ_3 ns	τ_4 ns	$\langle I(570) \rangle$	$\langle \alpha(570) \rangle$	τ_{rxn} ns	$\langle \tau_{rise} \rangle$ ns	$\langle \tau_{rxn} \rangle$ ns
T (K)	a_1	a_2	a_3	a_4									
274	-0.83	-1.19	2.89	0.13	<u>0.44</u>	0.26	1.72	6	0.032	7.92	1.83	0.33	1.39
283	-1.73	-1.24	3.94	0.04	<u>0.40</u>	0.22	1.37	6	0.041	7.12	1.32	0.32	1.05
293	-6.87	3.84	3.99	0.04	<u>0.36</u>	0.40	1.05	5	0.049	7.05	1.00		
303	-5.94		6.93	0.01	<u>0.33</u>		0.83	5	0.056	7.19	0.80		
314	-7.27		8.26	0.01	<u>0.30</u>		0.65	5	0.065	7.12	0.62		
323	-9.57		10.56	0.01	<u>0.28</u>		0.55	5	0.069	7.47	0.55		
333	-9.83		10.82	0.01	<u>0.26</u>		0.48	5	0.071	7.66	0.50		
344	-11.64		12.62	0.01	<u>0.25</u>		0.42	5	0.076	7.76	0.43		
										$\langle 7.41 \rangle$			

Underlined lifetimes indicate values constrained in the fit to the emission data. $\langle I(570) \rangle$ is the average value of the fluorescence intensity at 570 nm for the spectrum normalized to the peak intensity in the normal region. $\langle \alpha(570) \rangle$ is the calculated ratio of normal to tautomer radiative rates. τ_{rxn} is the calculated reaction time based on the irreversible proton-transfer scheme.

Table 5.3: Temperature Dependence of Tautomer Emission of 1AC in Ethylene Glycol-D₂

1AC / EG-D ₂		Original Fit		Tautomer		
T (K)	a ₁		a ₃		τ ₁ ns	τ ₃ ns
274	-1.57		2.57		0.46	4.97
283	-2.87		3.87		0.47	3.78
293	-0.21		1.21		0.42	3.51
303	-3.69		4.69		0.42	2.51
314	-4.11		5.11		0.40	2.06
324	-4.41		5.41		0.37	1.80
334	-4.73		5.73		0.34	1.62
345	-4.47		5.47		0.31	1.48

1AC / EG-D ₂		Alt. Fit #1		Tautomer							
T (K)	a ₁	a ₂	a ₃	a ₄	τ ₁ ns	τ ₂ ns	τ ₃ ns	τ ₄ ns	<I(570)>	<α(570)>	τ _{rxn} ns
274	-1.68		1.86	0.82	0.55		3.21	<u>10</u>	0.021	8.16	4.32
283	-2.93		3.38	0.55	0.49		3.30	<u>8</u>	0.025	5.97	3.26
293	-1.66		2.27	0.39	1.08		1.58	<u>8</u>	0.029	23.40	6.10
303	-3.75		4.55	0.19	0.45		2.30	<u>8</u>	0.033	5.87	2.23
314	-4.15		5.02	0.13	0.41		1.96	<u>8</u>	0.036	5.85	1.90
324	-4.45		5.37	0.08	0.38		1.75	<u>7</u>	0.036	5.96	1.72
334	-4.59		5.54	0.06	0.34		1.59	<u>7</u>	0.035	6.25	1.64
345	-4.40		5.35	0.04	0.32		1.46	<u>7</u>	0.034	6.30	1.52
										<6.05>	

1AC / EG-D ₂		Alt. Fit #2		Tautomer									
T (K)	a ₁	a ₂	a ₃	a ₄	τ ₁ ns	τ ₂ ns	τ ₃ ns	τ ₄ ns	<I(570)>	<α(570)>	τ _{rxn} ns	<τ _{rise} > ns	<τ _{rxn} > ns
274	-1.72	-0.23	1.98	0.97	<u>0.64</u>	0.20	2.83	<u>10</u>	0.021	10.86	4.31	0.59	3.94
283	-3.93	-0.61	4.41	1.13	<u>0.57</u>	0.09	2.87	<u>8</u>	0.025	8.02	3.22	0.51	2.86
293	-0.40	0.25	0.88	0.26	<u>0.51</u>	0.06	2.29	<u>8</u>	0.029	7.61	2.45		
303	-3.74		4.51	0.23	<u>0.46</u>		2.25	<u>8</u>	0.033	6.17	1.95		
314	-4.15		5.02	0.13	<u>0.41</u>		1.96	<u>8</u>	0.036	5.85	1.61		
324	-4.45		5.37	0.08	<u>0.38</u>		1.75	<u>7</u>	0.036	5.96	1.46		
334	-4.59		5.54	0.06	<u>0.34</u>		1.59	<u>7</u>	0.035	6.25	1.39		
345	-4.40		5.35	0.04	<u>0.32</u>		1.46	<u>7</u>	0.034	6.30	1.29		
										<7.13>			

Underlined lifetimes indicate values constrained in the fit to the emission data. <I(570)> is the average value of the fluorescence intensity at 570 nm for the spectrum normalized to the peak intensity in the normal region. <α(570)> is the calculated ratio of normal to tautomer radiative rates. τ_{rxn} is the calculated reaction time based on the irreversible proton-transfer scheme.

Table 5.4: Temperature Dependence of Tautomer Emission of 7AI in Ethylene Glycol

7AI / EG	Original Fit		Tautomer						
T (K)	a ₁	a ₂	a ₃	a ₄	τ ₁ ns	τ ₂ ns	τ ₃ ns	τ ₄ ns	<τ _{rise} > ns
275	-5.29	-0.74	7.03		0.58	0.11	1.06		0.52
283	-8.01	-0.89	9.90		0.48	0.08	0.87		0.44
294	-7.71	-0.60	9.32		0.35	0.04	0.76		0.32
303	-5.28		6.28		0.26		0.69		
314	-6.18		7.18		0.21		0.61		
323	-6.16		7.16		0.18		0.56		
333	-7.13		7.97	0.16	0.18		0.46	1.65	
343	-6.18		7.07	0.11	0.16		0.43	2.04	

7AI / EG	Alt. Fit #1		Tautomer								
T (K)	a ₁	a ₂	a ₃	a ₄	τ ₁ ns	τ ₂ ns	τ ₃ ns	τ ₄ ns	<I(570)>	<α(570)>	τ _{rxn} ns
275		-3.38	4.33	0.04		0.45	1.12	6	0.098	25.59	0.86
283		-4.99	5.95	0.04		0.41	0.89	6	0.131	16.66	0.52
294		-5.99	6.93	0.06		0.35	0.73	5	0.156	13.59	0.36
303		-5.86	6.80	0.06		0.27	0.66	5	0.192	12.51	0.26
314		-6.81	7.75	0.06		0.22	0.59	5	0.210	12.92	0.21
323		-7.30	8.23	0.06		0.19	0.54	5	0.227	12.73	0.18
333		-7.37	8.30	0.07		0.16	0.50	5	0.253	12.11	0.15
343		-6.38	7.31	0.06		0.14	0.45	5	0.262	12.03	0.13
										<13.2>	

7AI / EG	Alt. Fit #2		Tautomer									
T (K)	a ₁	a ₂	a ₃	a ₄	τ ₁ ns	τ ₂ ns	τ ₃ ns	τ ₄ ns	<I(570)>	<α(570)>	τ _{rxn} ns	<τ _{rise} > ns
275	-0.98	-10.84	12.73	0.09	0.10	0.67	0.94	6	0.098	14.20	0.74	0.62
283	-1.09	-10.45	12.46	0.08	0.07	0.49	0.84	6	0.131	13.07	0.50	0.45
294	-1.82	-15.68	18.37	0.13	0.03	0.35	0.74	5	0.156	13.38	0.37	0.32
303		-5.78	6.72	0.06		0.27	0.67	5	0.192	12.93	0.27	
314		-6.81	7.75	0.06		0.22	0.59	5	0.210	12.92	0.22	
323		-7.30	8.23	0.06		0.19	0.54	5	0.227	12.73	0.18	
333		-7.37	8.30	0.07		0.16	0.50	5	0.253	12.11	0.15	
343		-6.38	7.31	0.06		0.14	0.45	5	0.262	12.03	0.13	
										<12.9>		

Underlined lifetimes indicate values constrained in the fit to the emission data. <I(570)> is the average value of the fluorescence intensity at 570 nm for the spectrum normalized to the peak intensity in the normal region. <α(570)> is the calculated ratio of normal to tautomer radiative rates. τ_{rxn} is the calculated reaction time based on the irreversible proton-transfer scheme.

Table 5.5: Temperature Dependence of Tautomer Emission of 7AI in Ethylene Glycol-D₂

7AI / EG-D ₂		Original Fit		Tautomer		
T (K)		a ₂	a ₃		τ ₂ ns	τ ₃ ns
275		-3.69	4.69		0.65	2.09
283		-5.95	6.95		0.65	1.53
294		-7.97	8.97		0.62	1.17
303		-11.09	12.09		0.55	0.96
314		-12.31	13.31		0.46	0.83
324		-11.50	12.50		0.38	0.77
334		-11.30	12.30		0.34	0.70
344		-11.65	12.65		0.30	0.64

7AI / EG-D ₂		Alt. Fit #1			Tautomer						
T (K)	a ₁	a ₂	a ₃	a ₄	τ ₁ ns	τ ₂ ns	τ ₃ ns	τ ₄ ns	<I(570)>	<α(570)>	τ _{rxn} ns
275		-3.74	4.72	0.02		0.66	2.06	<u>7</u>	0.070	45.0	2.16
283		-7.78	8.62	0.16		0.72	1.35	<u>7</u>	0.083	22.6	1.19
294		-14.13	14.94	0.20		0.71	1.00	<u>7</u>	0.097	14.4	0.75
303		-18.69	19.53	0.16		0.62	0.85	<u>7</u>	0.109	12.5	0.57
314		-18.96	19.82	0.14		0.52	0.74	<u>7</u>	0.115	12.5	0.47
324		-13.52	14.41	0.12		0.43	0.70	<u>7</u>	0.122	13.5	0.42
334		-14.63	15.52	0.11		0.38	0.64	<u>7</u>	0.118	14.4	0.40
344		-14.38	15.28	0.10		0.33	0.59	<u>7</u>	0.121	14.8	0.35
										<13.7>	

7AI / EG-D ₂		Alt. Fit #2			Tautomer						
T (K)	a ₁	a ₂	a ₃	a ₄	τ ₁ ns	τ ₂ ns	τ ₃ ns	τ ₄ ns	<I(570)>	<α(570)>	τ _{rxn} ns
275	-0.84	24.73	-23.14	0.25	0.26	1.40	<u>1.18</u>	<u>7</u>	0.070	17.0	1.42
283		-33.59	34.37	0.22		0.93	<u>1.07</u>	<u>7</u>	0.083	13.9	0.92
294		-20.93	21.73	0.20		0.75	<u>0.95</u>	<u>7</u>	0.097	12.9	0.69
303		-17.55	18.39	0.16		0.62	<u>0.86</u>	<u>7</u>	0.109	12.8	0.56
314		-16.05	16.91	0.14		0.49	<u>0.77</u>	<u>7</u>	0.115	13.5	0.47
324		-13.52	14.41	0.12		0.43	<u>0.70</u>	<u>7</u>	0.122	13.5	0.41
334		-14.63	15.52	0.11		0.38	<u>0.64</u>	<u>7</u>	0.118	14.4	0.38
344		-14.38	15.28	0.10		0.33	<u>0.59</u>	<u>7</u>	0.121	14.8	0.34
										<14.1>	

Underlined lifetimes indicate values constrained in the fit to the emission data. <I(570)> is the average value of the fluorescence intensity at 570 nm for the spectrum normalized to the peak intensity in the normal region. <α(570)> is the calculated ratio of normal to tautomer radiative rates. τ_{rxn} is the calculated reaction time based on the irreversible proton-transfer scheme.

Table 5.6: Estimated Temperature Dependence of Quantum Yields and Radiative Rates for Normal 1AC in Ethylene Glycol and Ethylene Glycol- D₂

1AC / EG	ϕ (total)	ϕ (T)	ϕ (N)	τ (N) ns	$k_{\text{rad}}(\text{N})$ 10^7 s^{-1}
Temperature ($^{\circ}\text{C}$)					
1	0.033	0.0014	0.031	1.75	1.79
10	0.025	0.0013	0.023	1.37	1.71
20	0.019	0.0013	0.018	1.05	1.69
30	0.015	0.0012	0.014	0.82	1.68
40	0.012	0.0010	0.011	0.66	1.70
50	0.010	0.0009	0.009	0.55	1.73
60	0.009	0.0008	0.008	0.49	1.70
71	0.008	0.0008	0.007	0.43	1.70
mean:					$1.71 \pm 2\%$

1AC / EG-D ₂	ϕ (total)	ϕ (T)	ϕ (N)	τ (N) ns	$k_{\text{rad}}(\text{N})$ 10^7 s^{-1}
Temperature ($^{\circ}\text{C}$)					
1	0.078	0.0026	0.076	4.6	1.65
10	0.064	0.0022	0.062	3.6	1.71
20	0.051	0.0020	0.049	2.8	1.76
30	0.043	0.0019	0.041	2.37	1.75
40	0.036	0.0016	0.035	1.99	1.75
50	0.032	0.0014	0.031	1.75	1.77
60	0.030	0.0015	0.028	1.59	1.77
71	0.027	0.0013	0.026	1.51	1.69
mean:					$1.73 \pm 2\%$

The total quantum yields were estimated by scaling relative quantum yields to $\phi = 0.019$ at 20 $^{\circ}\text{C}$ for 1AC / EG and $\phi = 0.051$ at 20 $^{\circ}\text{C}$ for 1AC / EG-D₂ (*Table 2.3*). The extent of the tautomer emission band was estimated using a tautomer lineshape obtained from 1AC in benzyl alcohol.

Table 5.7: Estimated Reaction Rates for 1AC in Ethylene Glycol Based on the Irreversible Proton-Transfer Scheme

Temperature (°C)	Tautomer rise, ns	$k_{\text{rad}}(\text{T})$ 10^6 s^{-1}	$k_{\text{rad}}\text{N} / k_{\text{rad}}\text{T}$ α	k_{obs} 10^9 s^{-1}	k_{rxn} calculated 10^9 s^{-1}	k^{N} 10^9 s^{-1}	k_{rxn} calculated 10^9 s^{-1}	k^{N} 10^9 s^{-1}
Alt. fit #2					$\alpha = 5.2$		$\alpha = 9.0$	
1	0.44	3.2	5.6	0.57	0.53	0.043	0.91	-0.34
10	0.40	3.2	5.4	0.73	0.70	0.030	1.21	-0.48
20	0.36	3.6	4.7	0.95	1.04	-0.091	1.81	-0.85
30	0.33	3.6	4.6	1.22	1.37	-0.15	2.37	-1.1
40	0.30	3.4	5.1	1.52	1.56	-0.043	2.70	-1.2
50	0.28	3.1	5.6	1.82	1.70	0.12	2.94	-1.1
60	0.26	3.2	5.4	2.04	1.98	0.065	3.42	-1.4
71	0.25	3.1	5.5	2.33	2.20	0.13	3.80	-1.5
mean:		3.3 ± 0.2	5.2 ± 0.4					
Alt. fit #1					$\alpha = 4.8$		$\alpha = 9.0$	
1	0.31	4.5	4.0	0.57	0.69	-0.12	1.30	-0.73
10	0.30	4.2	4.1	0.73	0.86	-0.13	1.62	-0.89
20	0.32	4.0	4.2	0.95	1.08	-0.13	2.03	-1.1
30	0.31	3.8	4.4	1.22	1.34	-0.12	2.52	-1.3
40	0.30	3.4	5.1	1.52	1.44	0.077	2.70	-1.2
50	0.28	3.1	5.6	1.82	1.57	0.25	2.94	-1.1
60	0.26	3.2	5.4	2.04	1.82	0.22	3.42	-1.4
71	0.25	3.1	5.5	2.33	2.03	0.30	3.80	-1.5
mean:		3.7 ± 0.5	4.8 ± 0.6					
original fit					$\alpha = 4.7$		$\alpha = 9.0$	
1	0.31	4.5	4.0	0.57	0.68	-0.11	1.30	-0.73
10	0.30	4.2	4.1	0.73	0.84	-0.11	1.62	-0.89
20	0.31	4.1	4.1	0.95	1.10	-0.14	2.10	-1.1
30	0.31	3.8	4.4	1.22	1.32	-0.096	2.52	-1.3
40	0.29	3.5	4.9	1.52	1.46	0.059	2.79	-1.3
50	0.28	3.1	5.6	1.82	1.54	0.28	2.94	-1.1
60	0.26	3.2	5.4	2.04	1.79	0.25	3.42	-1.4
71	0.24	3.2	5.3	2.33	2.07	0.26	3.96	-1.6
mean:		3.7 ± 0.5	4.7 ± 0.6					

The observed rate k_{obs} is compared to calculated reaction rates. Two values of the ratio of normal to tautomer radiative rates (α) are tested: $\alpha \sim 5$ determined from EG data and $\alpha = 9$ from Table 2.3. The values of k^{N} provide an indication of the quality of the estimated rates, with negative values of k^{N} being nonphysical solutions.

Table 5.8: Estimated Reaction Rates for 1AC in Ethylene Glycol- D₂ Based on the Irreversible Proton-Transfer Scheme

Temperature (°C)	Tautomer rise, ns	$k_{\text{rad}}(\text{T})$ 10^6 s^{-1}	$k_{\text{rad}}^{\text{N}} / k_{\text{rad}}^{\text{T}}$ α	k_{obs} 10^9 s^{-1}	k_{rxn} calculated 10^9 s^{-1}	k^{N} 10^9 s^{-1}	k_{rxn} calculated 10^9 s^{-1}	k^{N} 10^9 s^{-1}
	Alt. fit #2				$\alpha = 4.4$		$\alpha = 9.0$	
1	0.64	4.0	4.1	2.17	2.32	-0.15	4.75	-2.6
10	0.57	3.9	4.4	2.78	2.77	0.0031	5.68	-2.9
20	0.51	3.9	4.6	3.57	3.45	0.13	7.05	-3.5
30	0.46	4.1	4.3	4.22	4.32	-0.10	8.84	-4.6
40	0.41	3.8	4.6	5.03	4.85	0.18	9.92	-4.9
50	0.38	3.8	4.7	5.71	5.38	0.33	11.0	-5.3
60	0.34	4.3	4.1	6.29	6.78	-0.49	13.9	-7.6
71	0.32	4.0	4.3	6.62	6.82	-0.20	14.0	-7.3
mean:		4.0 ± 0.2	4.4 ± 0.2					
	Alt. fit #1				$\alpha = 4.8$		$\alpha = 9.0$	
1	0.55	4.6	3.5	2.17	2.95	-0.77	5.53	-3.4
10	0.49	4.5	3.8	2.78	3.52	-0.74	6.60	-3.8
20	1.1	1.8	9.7	3.57	1.78	1.8	3.33	0.24
30	0.45	4.2	4.2	4.22	4.82	-0.60	9.04	-4.8
40	0.41	3.8	4.6	5.03	5.29	-0.26	9.92	-4.9
50	0.38	3.8	4.7	5.71	5.87	-0.16	11.0	-5.3
60	0.34	4.3	4.1	6.29	7.39	-1.1	13.9	-7.6
71	0.32	4.0	4.3	6.62	7.44	-0.82	14.0	-7.3
mean:		3.9 ± 0.8	4.8 ± 0.2					
	original fit				$\alpha = 3.9$		$\alpha = 9.0$	
1	0.46	5.6	3.0	2.17	2.86	-0.69	6.61	-4.4
10	0.47	4.7	3.6	2.78	2.98	-0.20	6.88	-4.1
20	0.42	4.7	3.8	3.57	3.71	-0.14	8.56	-5.0
30	0.42	4.5	3.9	4.22	4.20	0.023	9.68	-5.5
40	0.40	3.9	4.4	5.03	4.41	0.62	10.2	-5.1
50	0.37	3.9	4.5	5.71	4.90	0.82	11.3	-5.6
60	0.34	4.3	4.1	6.29	6.01	0.28	13.9	-7.6
71	0.31	4.1	4.1	6.62	6.24	0.38	14.4	-7.8
mean:		4.5 ± 0.5	3.9 ± 0.5					

The observed rate k_{obs} is compared to calculated reaction rates. Two values of the ratio of normal to tautomer radiative rates (α) are tested: $\alpha \sim 5$ determined from EG data and $\alpha = 9$ from Table 2.3. The values of k^{N} provide an indication of the quality of the estimated rates, with negative values of k^{N} being nonphysical solutions.

Table 5.9: Temperature Dependence of IAC Lifetimes in Benzyl Alcohol

	T (K)	a ₁	a ₂	a ₃	τ ₁ (ns)	τ ₂ (ns)	τ ₃ (ns)
Normal (λ _{em} =400 nm)	278.2	0.37	0.63		0.26	0.61	
	288.2	0.31	0.69	0.00	0.21	0.43	5.0
	298.2	1.00		0.01	0.30		1.6
	308.7	1.00		0.00	0.24		2.2
	318.2	0.99		0.01	0.20		3.2
	328.2	1.00		0.00	0.18		2.8
	338.2	0.99		0.01	0.16		3.0
	Tautomer (λ _{em} =560 nm)	278.2	-7.05	8.05		0.30	0.68
288.2		-11.67	12.67		0.28	0.53	
298.2		-15.57	16.56	0.00	0.25	0.45	10
308.7		-23.30	24.29	0.01	0.21	0.40	10
318.2		-38.85	39.82	0.03	0.18	0.37	10
328.2		-112.97	113.91	0.07	0.17	0.33	10
338.2		-228.87	229.72	0.15	0.15	0.31	10

Table 5.10: Estimated Temperature Dependence of Solute Rotation Times in Various Protic Solvents

	MeOH	1-PrOH	1-BuOH	BzOH	EG	PG	Water	FA	NMF
Viscosity (cP, 298K)	0.54	1.95	2.61	5.50	17.75	48.40	0.90	3.34	1.66
$(\eta / T) / (\eta_{298} / 298 \text{ K})$									
Temperature (K)									
223	6.1	14.2							
233	4.3	9.1							
243	3.2	6.0	8.3						
253	2.5	4.1	5.2						
263	2.0	2.9	3.4		6.6	15.6			
273	1.6	2.1	2.3	2.7	3.6	6.3	2.2	2.3	1.9
283	1.3	1.5	1.6	1.8	2.1	2.8	1.5	1.6	1.4
293	1.1	1.1	1.2	1.2	1.3	1.4	1.1	1.2	1.1
298	1.0	1.0	1.0	1.0	1.0	1.0	1.0	1.0	1.0
303	0.9	0.9	0.9	0.8	0.8	0.7	0.9	0.9	0.9
313	0.8	0.7	0.6	0.6	0.5	0.4	0.7	0.7	0.7
323	0.7	0.5	0.5	0.5	0.4	0.3	0.6	0.5	0.6
333	0.6	0.4	0.4	0.4	0.3	0.2	0.5	0.4	0.5
$\langle \tau_{\text{rot}} \rangle$ estimate 1AC, ps									
223	45	308							
233	32	197							
243	24	131							
253	18	89							
263	15	63							
273	12	45		225	655	3276	21	93	38
283	10	33		145	378	1469	15	65	29
293	8	25		99	230	720	11	47	22
298	7	22		83	183	519	10	40	20
303	7	19		70	147	381	8	35	18
313	6	15		51	98	216	7	26	14
323	5	12		38	68	130	5	21	12
333	4	9		30	49	83	4	17	10
$\langle \tau_{\text{rot}} \rangle$ estimate 7AI, ps									
223	31	210							
233	22	134							
243	16	89	173						
253	13	61	109						
263	10	43	72						
273	8	31	49		444	2229	14		
283	7	23	34		256	999	10		
293	5	17	24		156	490	7		
298	5	15	21		124	353	7		
303	5	13	18		100	259	6		
313	4	10	13		67	147	5		
323	3	8	10		46	89	4		
333	3	6	8		33	56	3		

Table 5.10 (continued)

Table Notes

The temperature dependence of viscosities were calculated according to the algorithms of (a) C. L. Yaws, *Handbook of Viscosity*. (Houston, Gulf Pub. Co., 1995). (b) D. S. Viswanath and G. Natarajan, *Data Book on the Viscosity of Liquids*. (New York, Hemisphere Pub. Corp., 1989).

Rotational times were estimated for 1AC and 7AI assuming the following values for C_{obs} [M. L. Horng, J. A. Gardecki, and M. Maroncelli, *J. Phys. Chem. A*, **101**, 1030 (1997)]: 0.64 (Methanol, MeOH), 0.52 (1-Propanol, 1-PrOH), 0.55 (1-Butanol, 1-BuOH), 0.7 (Benzyl Alcohol, BzOH), 0.48 (Ethylene Glycol, EG), 0.5 (Propylene Glycol, PG), 0.5 (Water), 0.56 (Formamide, FA), and 0.56 (N-Methylformamide, NMF). The calculations further assumed $f = 0.6$, $V_p(1AC) = 147 \text{ \AA}^3$, and $V_p(7AI) = 104 \text{ \AA}^3$.

The shaded regions indicate the onset of “anomalous” kinetic behavior of 1AC or 7AI. The regions not shaded in this table mean that experimental data are not available or that the observed kinetics are consistent with the simple irreversible proton-transfer scheme.

Table 5.11: Arrhenius Activation Energies (20 °C) for Solvent Properties and Reaction Rates of 1AC and 7AI

Solvent ⁽¹⁾	E(η) kJ/mol	E(τ_D) kJ/mol	1AC	7AI
			E _{act} kJ/mol	E _{act} kJ/mol
Methanol	10.9 ^a , 10.5 ^b	17 ± 2 ^k , 15.8 ^l	9.5 ^p	13 ^q , 9.9 ^b , 9.7 ^a
Ethanol	9.7 ^c , 11 ^d , 14.8 ^a		----	9.1 ^{cr} , 20 ^d , 16 ^q , 12.7 ^a
1-Propanol	18 ^d	20.5 ^l	12.6 ^p	26 ^d
1-Butanol	18 ^c , 29 ^d , 19.3 ^b		----	16 ^c , 31 ^d , 17.5 ^b
Benzyl Alcohol	21.4 ^e		~10	----
Ethylene Glycol	27.9 ^a , 31 ^{ce,f}	22 ^m , 29 ± 2 ^k	18	17 ^a , 20
Propylene Glycol	42 ^g	26 ^m	~21	~27
Water	15.5 ^h , 15 ⁱ	16 ± 1 or 12 ± 1 ⁿ	9.6	8.8 ⁱ , 10.3 ^{bs}
Formamide	19.5 ^e	13.8 ± 0.8 ^o , 17 ± 2 ^k	13	----
N-Methylformamide	14.2 ^j	9.1 ± 0.1 ^o	15	----

¹ Because the observed isotope effects are largely independent of temperature, the E_{act} do not differ greatly from the normal alcohols, diols, or water. Data for viscous solvents was fit for a small range about room temperature (~10 - 40 °C).

^a R. S. Moog and M. Maroncelli, *J. Phys. Chem.*, **95**, 10359 (1991).

^b M. Negreterie, F. Gai, S. M. Bellefeuille, and J. W. Petrich, *J. Phys. Chem.*, **95**, 8663 (1991).

^c H. Bulska, A. Grabowska, B. Pakula, J. Sepiol, J. Waluk, and U. P. Wild, *J. Lumin.*, **29**, 65 (1984).

^d J. Herbich, J. Sepiol, and J. Waluk, *J. Mol. Struct.*, **114**, 329 (1984).

^e Arrhenius fit to data in D. S. Viswanath and G. Natarajan, *Data Book on the Viscosity of Liquids*. (New York, Hemisphere Pub. Co., 1989).

^f Arrhenius fit to data in D. Bohne, S. Fischer, and E. Obermeier, *Ber. Bunsenges. Phys. Chem.*, **88**, 739 (1984).

^g Arrhenius fit to data in L. H. Thomas, R. Meatyard, H. Smith, and G. H. Davis, *J. Chem. Eng. Data*, **24**, 161 (1979); J. A. Riddick, W. B. Bunger, and T. K. Sakano, *Organic Solvents*. (New York, Wiley, 1986).

^h Y. Chen, R. L. Rich, F. Gai, and J. W. Petrich, *J. Phys. Chem.*, **97**, 1770 (1993).

ⁱ C. F. Chapman and M. Maroncelli, *J. Phys. Chem.*, **96**, 8430 (1992).

^j Arrhenius fit to data in C. L. Yaws, *Handbook of Viscosity*. (Houston, Gulf Pub. Co., 1995).

^k B. P. Jordan, R. J. Sheppard, and S. Szwarnowski, *J. Phys. D: Appl. Phys.*, **11**, 695 (1978).

^l Arrhenius fit to data compiled in E. W. Castner, Jr., B. Bagchi, M. Maroncelli, S. P. Webb, A. J. Ruggiero, and G. R. Fleming, *Ber. Bunsenges. Phys. Chem.*, **92**, 363 (1988).

^m A. El-Samahy, B. Gestblom, and J. Sjöblom, *Finn. Chem. Lett.*, **1984**, 54.

ⁿ Activation energies for 271-293 K and 315-367 K, respectively. C. Rønne, L. Thrane, P.-O. Åstrand, A. Wallqvist, K. V. Mikkelsen, and S. R. Keiding, *J. Chem. Phys.*, **107**, 5319 (1997).

^o S. M. Puranik, A. C. Kumbharkhane, and S. C. Mehrotra, *Ind. J. Chem.*, **32A**, 613 (1993).

^p S. J. Boryschuk, M. S. Thesis, The Pennsylvania State University, 1993.

^q J. Konijnenberg, A. H. Huizer, and C. A. G. O. Varma, *J. Chem. Soc., Faraday Trans. 2*, **84**, 1163 (1988).

^r J. Waluk, H. Bulska, B. Pakula, and J. Sepiol, *J. Lumin.*, **24/25**, 519 (1981).

^s A "short-lived" lifetime (~70 ps) has E_{act} = 2.7 ± 1.7 kcal/mol. [Y. Chen, R. L. Rich, F. Gai, and J. W. Petrich, *J. Phys. Chem.*, **97**, 1770 (1993).]

Table 5.12: Solvent Dielectric Relaxation Times

Solvent	$\langle\tau_{D1}\rangle$ (ps)	Reference	$\tau_{rxn}(1AC)$ (ps)
Primary Alcohols			
methanol	54	1,2	540
ethanol	191	1,2,3	790
1-propanol	430	1	770
1-butanol	581	1,4,5	860
1-pentanol	879	1,3	900
1-heptanol	1378	1,3	1210
1-octanol	1755	1,3	1160
1-nonanol	2030	1,3	1280
1-decanol	2115	1,3	1290
1-undecanol	1538	1	1060
benzyl alcohol	250	6	290
2-methyl-1-propanol			850
Secondary Alcohols			
2-propanol	411	2,7	1130
2-butanol	490	5	
3-pentanol			1590
cyclohexanol	2290	8	1340
Tertiary Alcohols			
2-methyl-2-propanol	331	4,9,10	1920
2-methyl-2-butanol	210	11	2210
3-ethyl-3-pentanol			3810
Diols			
ethylene glycol	143	3,12	940
propylene glycol	430	3,13	1860
Triols			
glycerol	1719	13	2640
Water	8.5	9,10,14	2320

Solvent (Debye) dielectric relaxation times measured at 20 or 25 °C are from the sources listed below:

1. Y. R. Kim, J. T. Yardley, and R. M. Hochstrasser, *Chem. Phys.*, **136**, 311-319 (1989).
2. D. Bertolini, M. Cassettari, and G. Salvetti, *J. Chem. Phys.*, **78**, 365-372 (1983).
3. B. Gestblom, A. El-Samahy, and J. Sjöblom, *J. Solution Chemistry*, **14**, 375-392 (1985).
4. S. M. Puranik, A. C. Kumbharkhane, and S. C. Mehrotra, *Indian J. Pure & Appl. Phys.*, **29**, 47-48 (1991).
5. H. A. Rizk and N. Youssef, *Z. Phys. Chem. (Frankfurt am Main)*, **58**, 100-113 (1968).
6. V. A. Durov, C. Puchala, M. I. Shakhpsaronov, and N. V. Lifanova, *Russ. J. Phys. Chem.*, **57**, 1367-1369 (1983).
7. J. Barthel, *DECHEMA Chemistry Data Series, Vol 12: Electrolyte Data Collection, Part 2a: Nonaqueous Solutions* (DECHEMA, Frankfurt, 1995).
8. S. K. Garg and C. P. Smyth, *J. Chem. Phys.*, **46**, 373 (1967).
9. S. Mashimo and N. Miura, *J. Chem. Phys.*, **99**, 9874-9881 (1993).
10. A. C. Kumbharkhane, S. M. Puranik, and S. C. Mehrotra, *J. Chem. Soc. Faraday Trans.*, **87**, 1569-1573 (1991).
11. A. D'Apprano, I. D. Donato, G. D'Arrigo, D. Bertolini, M. Cassettari, and G. Salvetti, *Mol. Phys.*, **55**, 475-488 (1985).
12. A. El-Samahy, B. Gestblom, and J. Sjöblom, *Finn. Chem. Lett.*, **1984**, 54.
13. A. Lux and M. Stockhausen, *Phys. Chem. Liquids*, **26**, 67-83 (1993) report the Cole-Davidson form of the dielectric relaxation: $\tau_{av} = 432$ ps for propylene glycol and $\tau_{av} = 1719$ ps for glycerol.
14. C. Rønne, L. Thrane, P. Åstrand, A. Wallqvist, K. V. Mikkelsen, and S. R. Keiding, *J. Chem. Phys.*, **107**, 5319, (1997).

The observed reaction rates for 1AC in these solvents are listed for comparison. Most of the data is from S. J. Boryschuk, M. S. Thesis, The Pennsylvania State University, 1993.

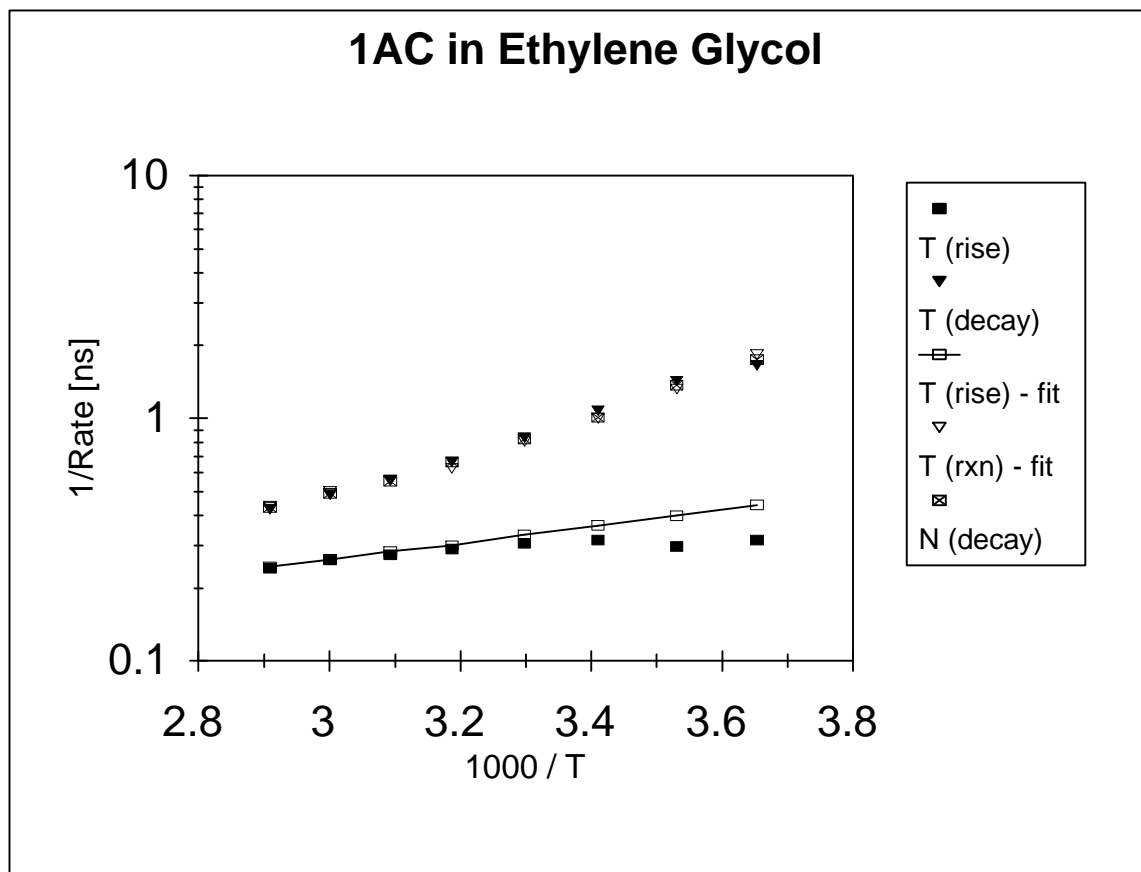


Figure 5.1: Temperature Dependence of 1AC Lifetimes in Ethylene Glycol

Lifetimes from an unconstrained fit (filled symbols) as well as from alternative fit #2 (open symbols) to the tautomer emission are shown.

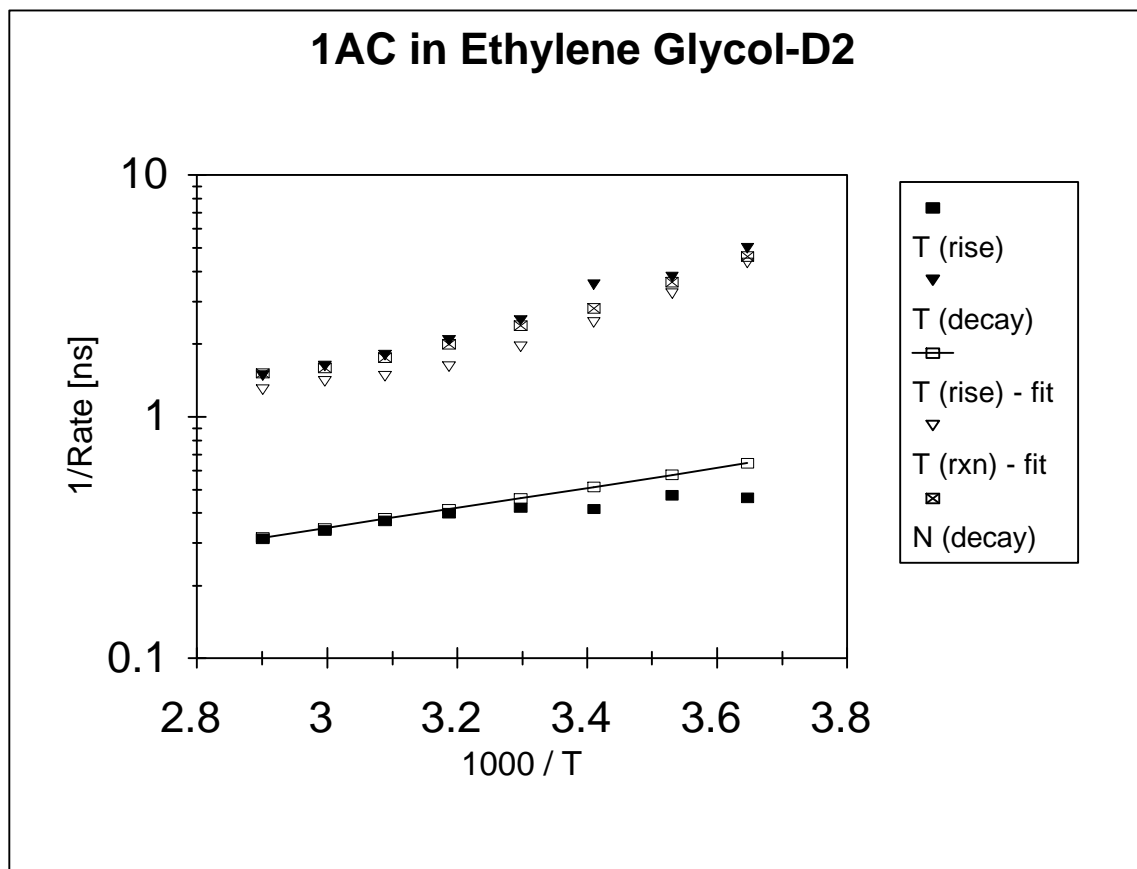


Figure 5.2: Temperature Dependence of 1AC Lifetimes in Ethylene Glycol-D₂

Lifetimes from an unconstrained fit (filled symbols) as well as from alternative fit #2 (open symbols) to the tautomer emission are shown.

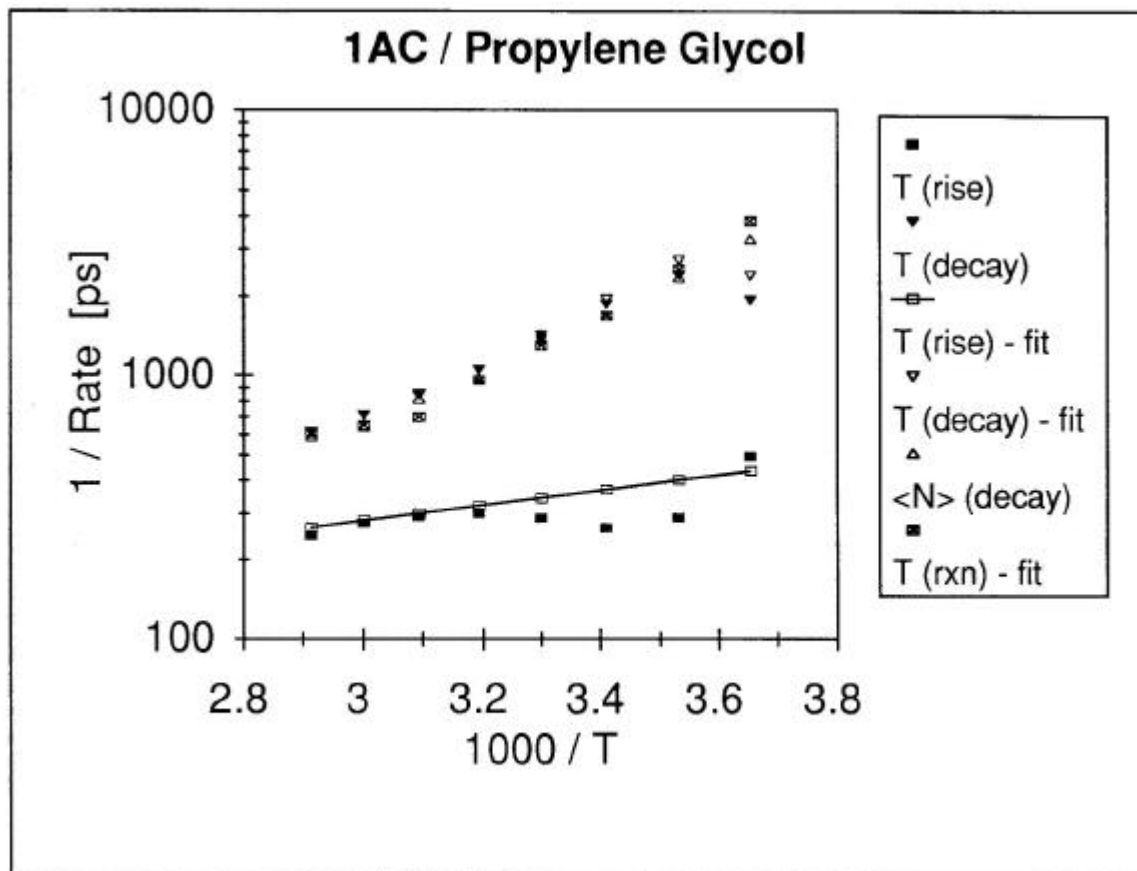


Figure 5.3: Temperature Dependence of 1AC Lifetimes in Propylene Glycol

Lifetimes from an unconstrained fit (filled symbols) as well as from alternative fit #2 (open symbols) to the tautomer emission are shown.

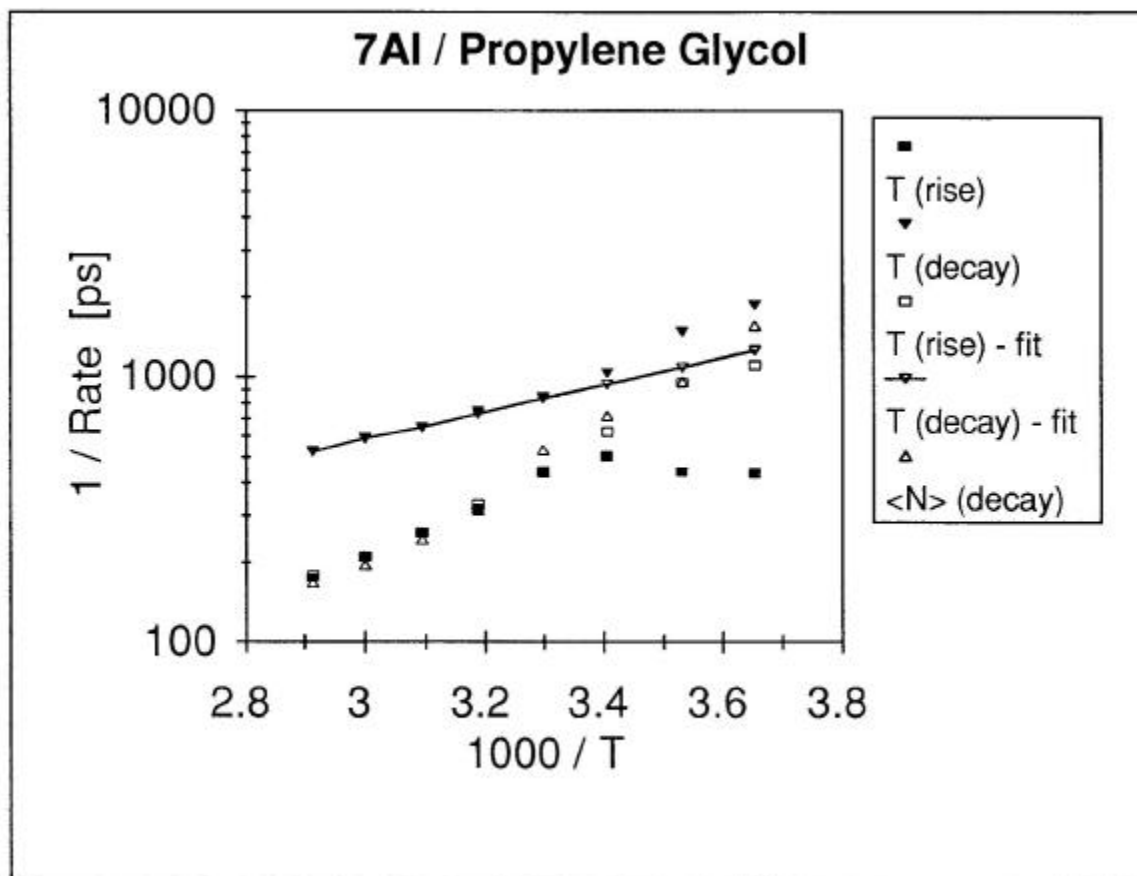


Figure 5.4: Temperature Dependence of 7AI Lifetimes in Propylene Glycol

Lifetimes from an unconstrained fit (filled symbols) as well as from alternative fit #2 (open symbols) to the tautomer emission are shown.

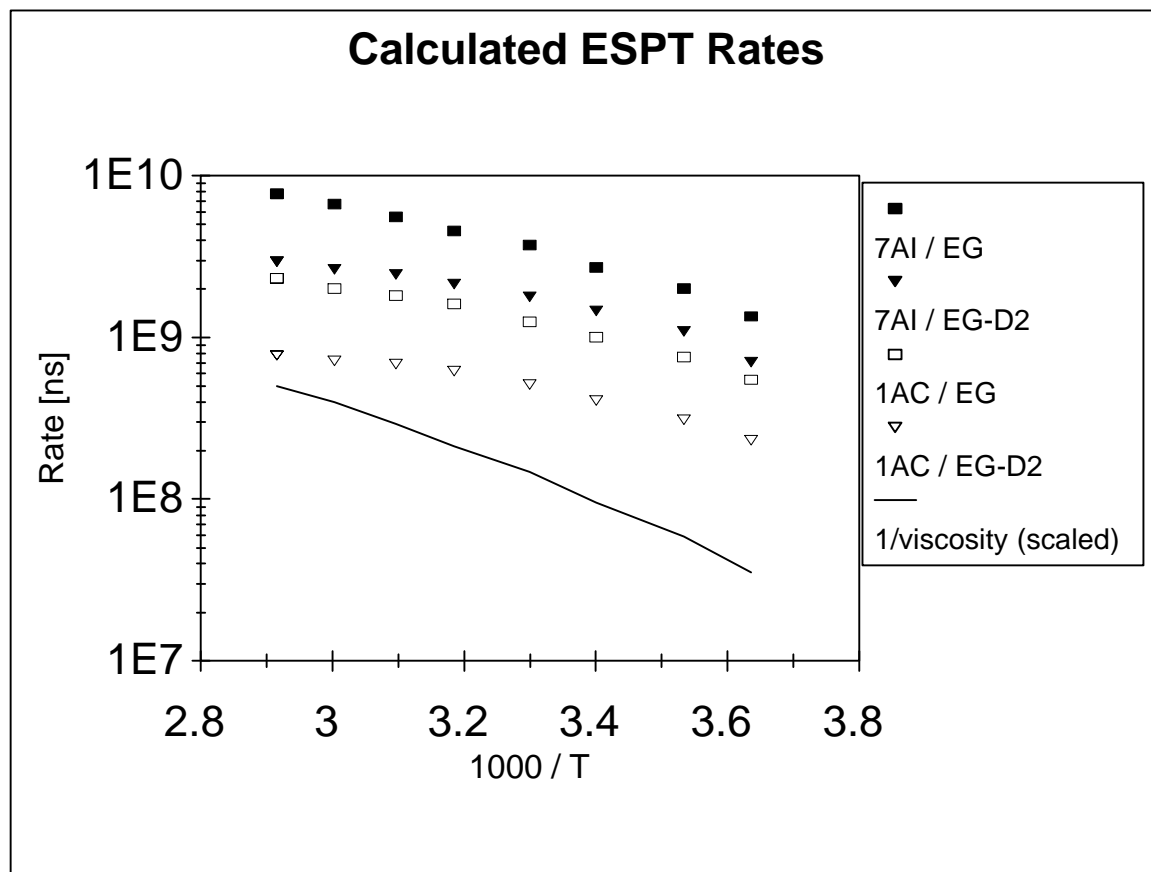


Figure 5.5: Summary of Temperature Dependence of Reaction Rates of 7AI and 1AC in Ethylene Glycol

The reaction rates were determined using “alternative fit #2” discussed in Section 5.2. The temperature dependence of the viscosity of ethylene glycol is shown for comparison. [Viscosity data from (a) D. S. Viswanath and G. Natarajan, *Data Book on the Viscosity of Liquids*. (New York, Hemisphere Pub. Co., 1989). (b) D. Bohne, S. Fischer, and E. Obermeier, *Ber. Bunsenges. Phys. Chem.*, **88**, 739, (1984).]

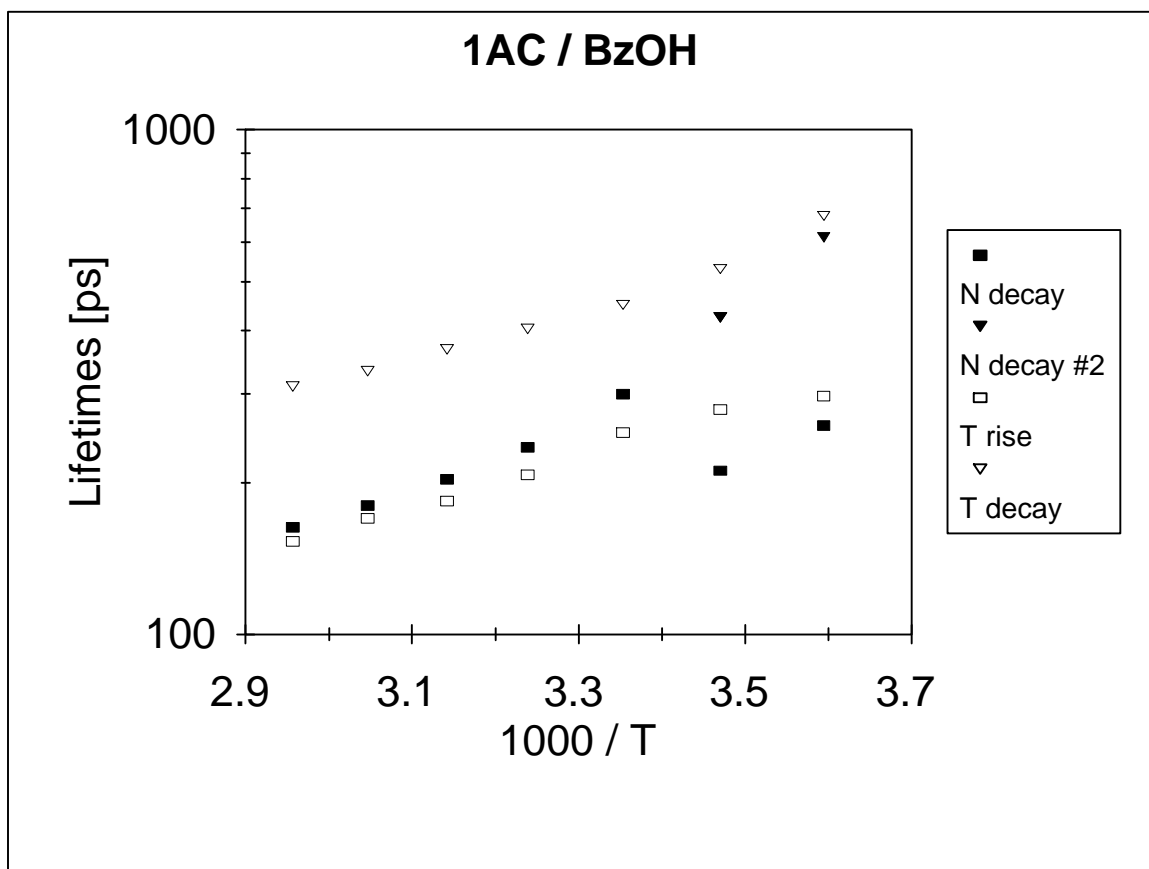


Figure 5.6: Temperature Dependence of 1AC in Benzyl Alcohol

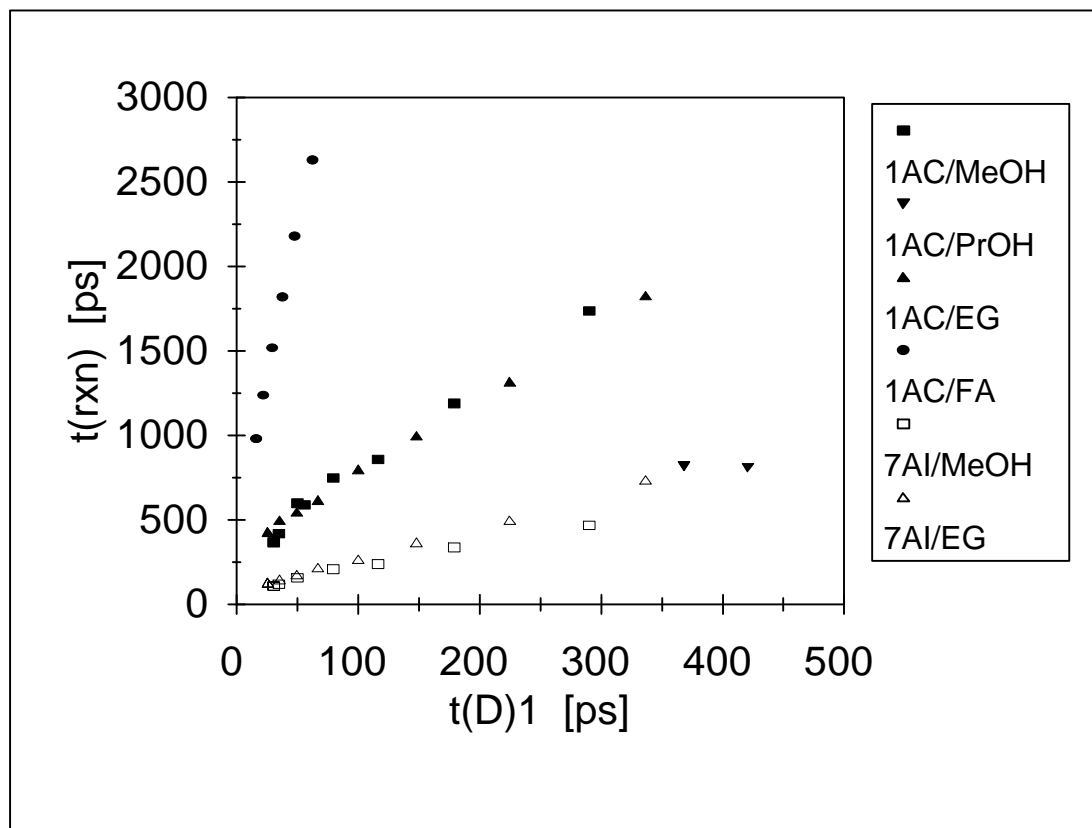


Figure 5.7: Comparison of Observed Rates and Solvent Dielectric Times (τ_1)

The reaction rate data in methanol and 1-propanol is from S. J. Boryschuk, M.S. Thesis, The Pennsylvania State University, 1993. Sources of the dielectric data used here are noted in Section 5.4 (Endnote 52).

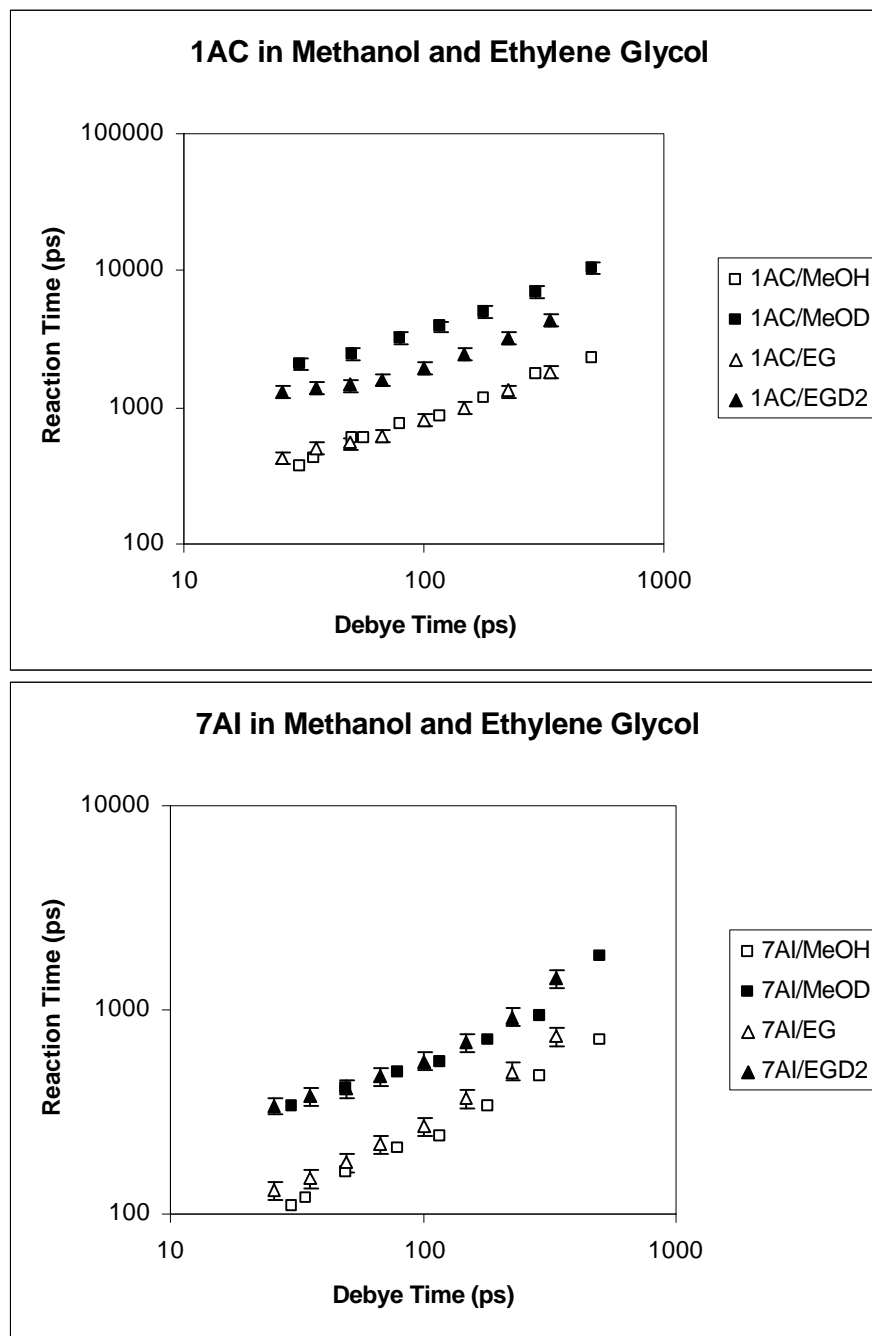


Figure 5.8: Isotope Effects in the Correlation between Reaction Rates and Solvent Dielectric Relaxation Times for 1AC and 7AI

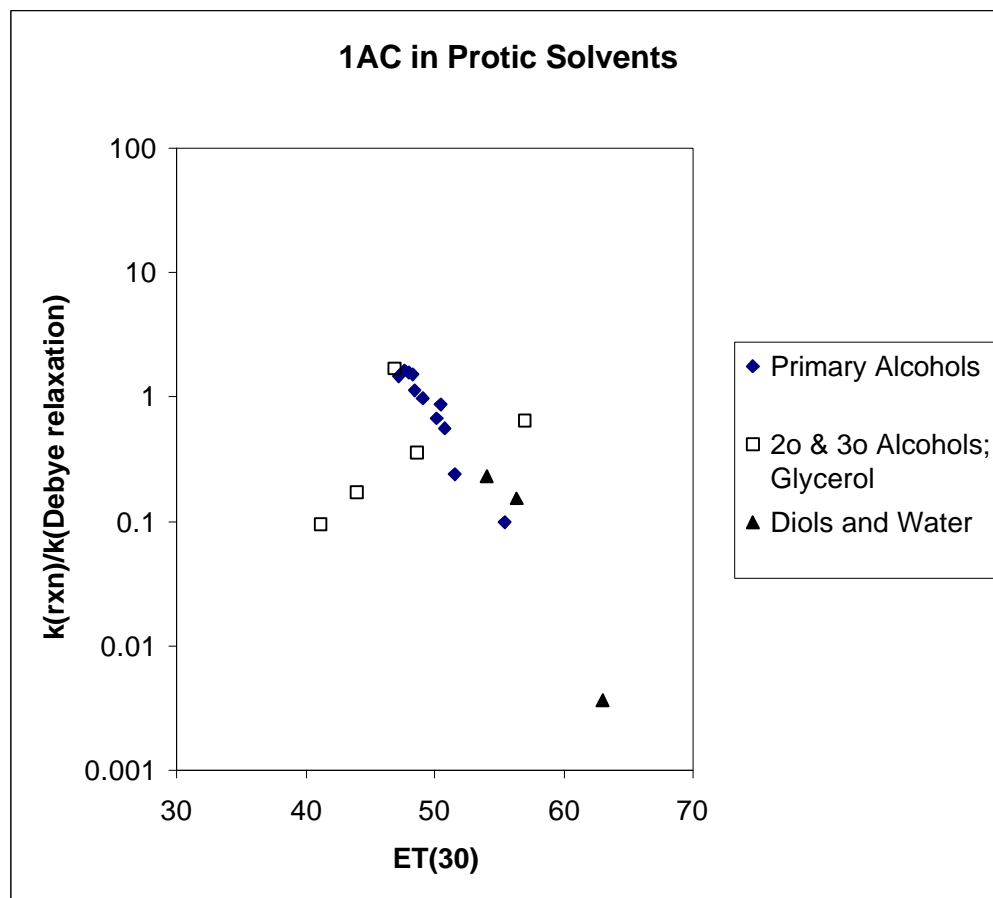


Figure 5.9: Solvent Dependence of 1AC Reaction Rates Normalized by a Measure of Hydrogen-Bond Lifetimes

ENDNOTES

- ¹ P. Avouris, L. L. Yang, and M. A. El-Bayoumi, *Photochem. Photobiol.*, **24**, 211 (1976).
- ² K. C. Ingham and M. A. El-Bayoumi, *J. Am. Chem. Soc.*, **96**, 1674 (1974).
- ³ C. A. Taylor, M. A. El-Bayoumi, and M. Kasha, *Proc. Nat. Acad. Sci. USA*, **63**, 253 (1969).
- ⁴ C. Chang, N. Shabestary, and M. A. El-Bayoumi, *Chem. Phys. Lett.*, **75**, 107 (1980).
- ⁵ H. Bulska, A. Grabowska, B. Pakula, J. Sepiol, J. Waluk, and U. P. Wild, *J. Lumin.*, **29**, 65 (1984).
- ⁶ J. Herbich, J. Sepiol, and J. Waluk, *J. Mol. Struct.*, **114**, 329 (1984).
- ⁷ J. Waluk, H. Bulska, B. Pakula, and J. Sepiol, *J. Lumin.*, **24/25**, 519 (1981).
- ⁸ H. Bulska and A. Chodkowska, *J. Am. Chem. Soc.*, **102**, 3259 (1980).
- ⁹ J. Waluk, S. J. Komorowski, and J. Herbich, *J. Phys. Chem.*, **90**, 3868 (1986).
- ¹⁰ S. Mente and M. Maroncelli, *J. Phys. Chem. A*, **102**, 3860-3876 (1998).
- ¹¹ See pp. 2761-2762 of A. V. Smirnov, D. S. English, R. L. Rich, J. Lane, L. Teyton, A. W. Schwabacher, S. Luo, R. W. Thornburg, and J. W. Petrich, *J. Phys. Chem. B.*, **101**, 2758 (1997).
- ¹² C. F. Chapman, T. J. Marrone, R. S. Moog, and M. Maroncelli, *Ultrafast Phenomena VIII* (Springer Series in Chemical Physics, Vol. 55), (J.-L. Martin, A. Mingus, G. A. Mourou, and A. H. Zewail, eds.) (Berlin: Springer-Verlag, 1993). pp. 624-625.
- ¹³ S. J. Boryschuk, M.S. Thesis, The Pennsylvania State University, 1993.
- ¹⁴ C. F. Chapman, Ph. D. Thesis, The Pennsylvania State University, 1993.
- ¹⁵ C. F. Chapman and M. Maroncelli, *J. Phys. Chem.*, **96**, 8430-8441 (1992).
- ¹⁶ R. S. Moog and M. Maroncelli, *J. Phys. Chem.*, **95**, 10359-10369 (1991).

- ¹⁷ R. S. Moog, S. C. Bovino, and J. D. Simon, *J. Phys. Chem.*, **92**, 6545-6547 (1988).
- ¹⁸ A. V. Smirnov, D. S. English, R. L. Rich, J. Lane, L. Teyton, A. W. Schwabacher, S. Luo, R. W. Thornburg, and J. W. Petrich, *J. Phys. Chem. B.*, **101**, 2758 (1997).
- ¹⁹ R. L. Rich, F. Gai, Y. Chen, and J. W. Petrich, *SPIE*, **2137**, 435 (1994).
- ²⁰ Y. Chen, F. Gai, and J. W. Petrich, *Chem. Phys. Lett.*, **222**, 329 (1994).
- ²¹ Y. Chen, F. Gai, and J. W. Petrich, *J. Phys. Chem.*, **98**, 2203 (1994).
- ²² F. Gai, R. L. Rich, and J. W. Petrich, *J. Am. Chem. Soc.*, **116**, 735 (1994).
- ²³ Y. Chen, F. Gai, and J. W. Petrich, *J. Am. Chem. Soc.*, **115**, 10158 (1993).
- ²⁴ Y. Chen, R. L. Rich, F. Gai, and J. W. Petrich, *J. Phys. Chem.*, **97**, 1770 (1993).
- ²⁵ M. Negrerie, F. Gai, J.-C. Lambry, J.-L. Martin, and J. W. Petrich, *Ultrafast Phenomena VIII* (Springer Series in Chemical Physics, Vol. 55), (J.-L. Martin, A. Mingus, G. A. Mourou, and A. H. Zewail, eds.) (Berlin: Springer-Verlag, 1993). pp. 621-623.
- ²⁶ M. Negrerie, F. Gai, J.-C. Lambry, J.-L. Martin, and J. W. Petrich, *J. Phys. Chem.*, **97**, 5046 (1993).
- ²⁷ R. L. Rich, Y. Chen, D. Neven, M. Negrerie, F. Gai, and J. W. Petrich, *J. Phys. Chem.*, **97**, 1781 (1993).
- ²⁸ F. Gai, Y. Chen, and J. W. Petrich, *J. Am. Chem. Soc.*, **114**, 8343 (1992).
- ²⁹ M. Negrerie, F. Gai, M. Bellefeuille, and J. W. Petrich, *J. Phys. Chem.*, **95**, 8663 (1991).
- ³⁰ M. Negrerie, S. M. Bellefeuille, S. Whitham, J. W. Petrich, and R. W. Thornburg, *J. Am. Chem. Soc.*, **112**, 7419 (1990).
- ³¹ P.-T. Chou, M. L. Martinez, W. C. Cooper, D. McMorro, S. T. Collins, and M. Kasha, *J. Phys. Chem.*, **96**, 5203 (1992).
- ³² S. T. Collins, *J. Phys. Chem.*, **87**, 3202 (1983).

³³ J. Konijnenberg, A. H. Huizer, and C. A. G. O. Varma, *J. Chem. Soc., Faraday Trans. 2.*, **84**, 1163 (1988).

³⁴ D. McMorro and T. J. Aartsma, *Chem. Phys. Lett.*, **125**, 581 (1986).

³⁵ T. Suzuki, U. Okuyama, and T. Ichimura, *J. Phys. Chem. A.*, **101**, 7047 (1997).

³⁶ K. S. Pandey and P. C. Mishra, *Indian J. Pure & Applied Phys.*, **31**, 727 (1993).

³⁷ Early absorption work reporting the photophysical and chemical properties of 7AI includes:

(a) M. M. Robinson and B. L. Robinson, *J. Am. Chem. Soc.*, **77**, 6554 (1955).

(b) T. K. Adler and A. Albert, *J. Chem. Soc.*, 1794 (1960).

(c) V. M. Clark, A. Cox, and E. J. Herbert, *J. Chem. Soc. C*, **1968**, 831.

(d) L. Stephenson and W. K. Warburton, *J. Chem. Soc. C*, **1970**, 1355.

³⁸ In an early study of the excited-state tautomerization reaction of 1AC in bulk alcohols, Waluk and coworkers suggested that at least two types of ground-state solvation structures could account for the kinetics observed with limited time-resolution. (Endnote 9)

³⁹ In an abstract, D. McMorro may indicate that the intrinsic proton transfer rate is even shorter (D. McMorro, *Bull. Am. Phys. Soc.*, **33**, 1635 (1988).)

⁴⁰ Preliminary measurements of 1AC in bulk primary, secondary, and tertiary amines reveal photophysical and photochemical behavior again different than that observed for 1AC in bulk alcohols. The amines [butylamine, diethylamine, and triethylamine] were distilled immediately prior to use to remove significant fluorescence impurities and natural oxidation products. In these weakly associating, hydrogen-bonded solvents, the normal form of 1AC is quenched rapidly (~10-20 ps) and little steady-state emission is observed. Emission in the region where the tautomer is expected to fluoresce is observed (rise time too rapid to measure, decay times ~0.43 - 0.49 ns). At slightly lower temperatures (1 °C), the reaction remains too rapid to measure well. The triethylamine was intended to be a control solvent in which no reaction is expected, but it is possible that trace impurities catalyzed the reaction anyway.

⁴¹ A scaled lineshape of a fit of the tautomer emission in benzyl alcohol was used to estimate the extent of the tautomer band in these determinations, as practiced for the

quantum yield values listed in Chapter 2, but unlike the use of discrete intensities applied in the earlier temperature work reported in *Table 5.2*, *Table 5.3*, *Table 5.4*, and *Table 5.5*. The quantum yield ratios determined for this work in *Table 5.6* differ from those in Chapter 2 because two different emission instrument correction files were used over the time in which the measurements were made.

⁴² An empirical expression involving a stretched exponential $N(t) = N(0)\exp[-(kt)^\beta]$ has been found useful for representing dispersive kinetics in glassy solvents. See the discussion in W. Siebrand and T. A. Wildman, *Acc. Chem. Res.*, **19**, 238, (1986) for an introduction.

⁴³ The origin of the dynamic Stokes shift is solvent reorganization about a different charge distribution of the excited-state solute. The dominant dielectric relaxation times of the neat solvents are measured to be EG, $\tau_1 = 145$ ps, and PG, $\tau_1 = 430$ ps, at 20 °C. [A. El-Samahy, B. Gestblom and J. Sjöblom, *Finn. Chem. Lett.*, **1984**, 54. B. Gestblom, A. El-Samahy, and J. Sjöblom, *J. Solution Chem.*, **14**, 375 (1985).] The longitudinal relaxation time, $\tau_L = (\epsilon_\infty / \epsilon_0) \tau$, may be a better indication of solvation dynamics times: EG, $\tau_L \sim 13$ ps, and PG, $\tau_L \sim 57$ ps.

⁴⁴ A. J. Benigno, E. Ahmed, and M. Berg, *J. Chem. Phys.*, **104**, 7382 (1996).

⁴⁵ J. H. Noggle, *Physical Chemistry, Second Edition* (Glenview, Illinois: Scott, Foresman and Company, 1989).

⁴⁶ M. L. Horng, J. A. Gardecki, and M. Maroncelli, *J. Phys. Chem. A*, **101**, 1030 (1997).

⁴⁷ A. Bondi, *J. Phys. Chem.*, **68**, 441 (1964).

⁴⁸ J. T. Edwards, *J. Chem. Ed.*, **47**, 261 (1970).

⁴⁹ C. L. Yaws, *Handbook of Viscosity*. (Houston, Gulf Pub. Co., 1995).

⁵⁰ D. S. Viswanath and G. Natarajan, *Data Book on the Viscosity of Liquids*. (New York, Hemisphere Pub. Corp., 1989).

⁵¹ As proposed earlier in the coumarin 153 rotational study: “...the comparable rotational behavior...in protic and polar aprotic solvents reflects a similarity in the hydrogen-bonding statics/dynamics between the solute and solvent and between molecules in the neat solvent itself.” [Endnote 46].

⁵² Using Dielectric relaxation times compiled in:

(a) E. W. Castner, Jr., B. Bagchi, M. Maroncelli, S. P. Webb, A. J. Ruggiero, and G. R. Fleming, *Ber. Bunsenges. Phys. Chem.*, **92**, 363 (1988).

(b) B. P. Jordan, R. J. Sheppard, and S. Szwarnowski, *J. Phys. D: Appl Phys.*, **11**, 695 (1978).

(c) S. M. Puranik, A. C. Kumbharkhane, and S. C. Mehrotra, *Indian J. Chem.*, **32A**, 613 (1993).

(d) J. Barthel and R. Buchner, *Pure & Appl. Chem.*, **63**, 1473 (1991).

Discussions of the interpretation of the multiple relaxation times include:

(a) S. K. Garg and C. P. Smyth, *J. Phys. Chem.*, **69**, 1294 (1965).

(b) E. Jakusek and L. Sobczyk, "Some Dielectric Studies of Molecular Association." in *Specialist Periodical Report: Dielectric and Related Molecular Processes, Volume 3*. (M. Davies, Ed.) (London, The Chemical Society, 1977). pp. 108-142.

⁵³ See, for example, C. Reichardt, *Solvents and Solvent Effects in Organic Chemistry, Second Revised and Enlarged Edition*, (New York, VCH, 1988).